



ELSEVIER

Contents lists available at SciVerse ScienceDirect

## Earth and Planetary Science Letters

journal homepage: [www.elsevier.com/locate/epsl](http://www.elsevier.com/locate/epsl)

## Water in volcanic pyroclast: Rehydration or incomplete degassing?

T. Giachetti\*, H.M. Gonnermann

Department of Earth Science, Rice University, P.O. Box 1892, Houston, TX 77005, USA

## ARTICLE INFO

## Article history:

Received 22 August 2012

Received in revised form

19 February 2013

Accepted 24 March 2013

Editor: T. Elliot

## Keywords:

magma

degassing

rehydration

diffusion

water

modeling

## ABSTRACT

The matrix-glass water concentrations in samples from volcanic eruptions of intermediate to highly silicic magmas were measured and compiled. They range from 0.1 wt% to more than 3.5 wt% and show a positive correlation with vesicles surface area over glass volume ratio. Modeling of water diffusion suggests that most of this correlation can be explained by the post-eruptive diffusion of external water at atmospheric temperature and pressure into the matrix-glass, a process referred to as rehydration. Although the precise proportion of primary (magmatic) to secondary (meteoric) water is not determined by our analysis, we find that most samples can be modeled by progressive rehydration of an initially 'dry' sample during the time interval between deposition and sample collection at an average rehydration diffusivity of approximately  $10^{-23} \text{ m}^2 \text{ s}^{-1}$ . This diffusivity estimate is consistent with values provided in the literature on obsidian hydration dating and with the extrapolation of diffusivity formulations for silicic melts to lower temperatures and pressures.

Published by Elsevier B.V.

## 1. Introduction

Explosive volcanism, if not caused by the interaction of magma with phreatic water, is largely a consequence of the exsolution of magmatic volatiles, predominantly water during volcanic eruptions involving intermediate to silicic magmas. Pre-eruptive water concentrations in andesite to rhyolite melts – estimated from melt inclusions (Anderson, 1974; Lowenstern, 1995, 2003; Sobolev, 1996; Schiano, 2003) or by experimental reproduction of mineral phase assemblages (Rutherford et al., 1985; Barclay et al., 1998; Hammer and Rutherford, 2002) – range between 4 and 6 wt% (Bacon et al., 1992; Johnson et al., 1994; Blundy and Cashman, 2005; Wallace, 2005; Blundy et al., 2006). Because water solubility is pressure-dependent, water exsolves into bubbles as magma rises to the surface and pressure decreases (Burnham, 1975; Silver and Stolper, 1985; Blank et al., 1993; Holloway and Blank, 1994; Moore et al., 1995, 1998; Papale, 1997, 1999; Zhang, 1999; Newman and Lowenstern, 2002; Liu et al., 2005; Papale et al., 2006; Zhang et al., 2007). Pressure dependent water solubility, together with a molar volume that is approximately proportional to pressure, requires that the erupted magma reaches porosities of > 99% if bubbles are free to expand and water exsolution proceeds at or near equilibrium in a closed-system. During most volcanic eruptions neither of these conditions are met.

Volcanic rocks often provide the only direct and accessible record of magma ascent, because in-situ observations of magma ascent are difficult, if not impossible. In particular, the volatile concentration of volcanic glass, the volume fraction of vesicles, as well as the vesicle size and shape constitute important measurable quantities that can be used to constrain magma ascent conditions (e.g., Toramaru, 1990; Klug and Cashman, 1994, 1996; Klug et al., 2002; Adams et al., 2006; Houghton et al., 2010; Giachetti et al., 2010; Shea et al., 2012; Moitra et al., 2013). It is the departure from the aforementioned ideal conditions that are thought to be of critical importance in determining or modulating the eruptive style, which may range from relatively quiescent magma effusion to violently destructive explosive behavior.

For example, if the exsolved volatiles cannot expand as fast as the confining pressure of the ascending magma decreases, bubbles may be at substantially higher pressure than the surrounding magma, possibly resulting in magma fragmentation and an explosive eruption (e.g., Sparks, 1978, 2003; Wilson, 1980; Zhang, 1999; Spieler et al., 2004; Namiki and Manga, 2005; Gonnermann and Manga, 2007; Mueller et al., 2008). In this case the magma fragments may have dissolved water concentrations that are higher and vesicularities that are lower than magma that ascends to the surface in a closed system and without fragmenting. By the same token, effusively erupting magma may undergo significant open-system degassing, thought to be a consequence of permeable flow through a network of interconnected bubbles and/or fractures (e.g., Eichelberger et al., 1986; Woods and Koyaguchi, 1994;

\* Corresponding author. Tel.: +1 832 454 0562.  
E-mail address: [tg10@rice.edu](mailto:tg10@rice.edu) (T. Giachetti).

Gonnermann and Manga, 2003; Rust and Cashman, 2004, 2011; Rust et al., 2004; Burgisser and Gardner, 2005; Melnik and Sparks, 2005; Mueller et al., 2005; Namiki and Manga, 2005; Okumura et al., 2009), resulting in low water concentrations and low vesicularities.

However, open-system degassing may not be limited to effusively erupting magma. For example, it plays an important role during Vulcanian eruptions, where the pre-eruptive emplacement of the magmatic column under partly open-system degassing conditions results in the formation of a 'plug' of dense, relatively water-poor magma (Clarke et al., 2007; Wright et al., 2007; Giachetti et al., 2010; Burgisser et al., 2010). During explosive eruptions, open-system degassing may also take place after the magma has fragmented into pyroclasts (Jaupart and Allègre, 1991; Thomas et al., 1994; Gardner et al., 1996) and some water may even diffuse from bubbles back into the melt prior to quenching in a process referred to as 'bubble resorption', probably resulting from an increase of water solubility with decreasing temperatures (Westrich and Eichelberger, 1994; Yoshimura and Nakamura, 2008, 2010; Watkins et al., 2012; McIntosh et al., 2013). Thus, the matrix-glass water concentration, as well as vesicle abundance, size, and shape of volcanic rocks represent an integrated record of the degassing processes during volcanic eruptions.

In this paper, we provide a comprehensive compilation, augmented by additional sample collection and analyses, of matrix-glass water concentrations and porosities in samples from

eruptions of intermediate to highly silicic magmas. We find a broad positive correlation between matrix-glass water concentration and the ratio of vesicle surface area to matrix-glass volume. This correlation is perplexing and counterintuitive, and a key question is whether, or to what extent, it reflects syn-eruptive conditions, in particular disequilibrium degassing. An alternate possibility could be that most of these samples have undergone some degrees of post-eruptive rehydration. To complement the few existing isotopic studies aimed at distinguishing between magmatic and meteoric water in volcanic glasses (e.g., Newman et al., 1988; DeGroat-Nelson et al., 2001; Nolan and Bindeman, in press), we use diffusion modeling to test the hypothesis that post-eruptive rehydration of dry glasses can explain the observed data.

## 2. Observed matrix-glass water concentration vs. sample porosity

In Fig. 1, we have compiled published matrix-glass water concentrations,  $C_s$ , in samples from volcanic eruptions of intermediate to highly silicic magmas. These data include 33 eruptions of 17 volcanic edifices with time intervals between eruption and analysis ranging from 6 months to 39,000 yr (see Table 1 for data and sources), and a large range of eruptive styles, from dome forming to Plinian eruptions. In addition, we have added 10 new measurements of pumices and obsidians from the 1110 AD

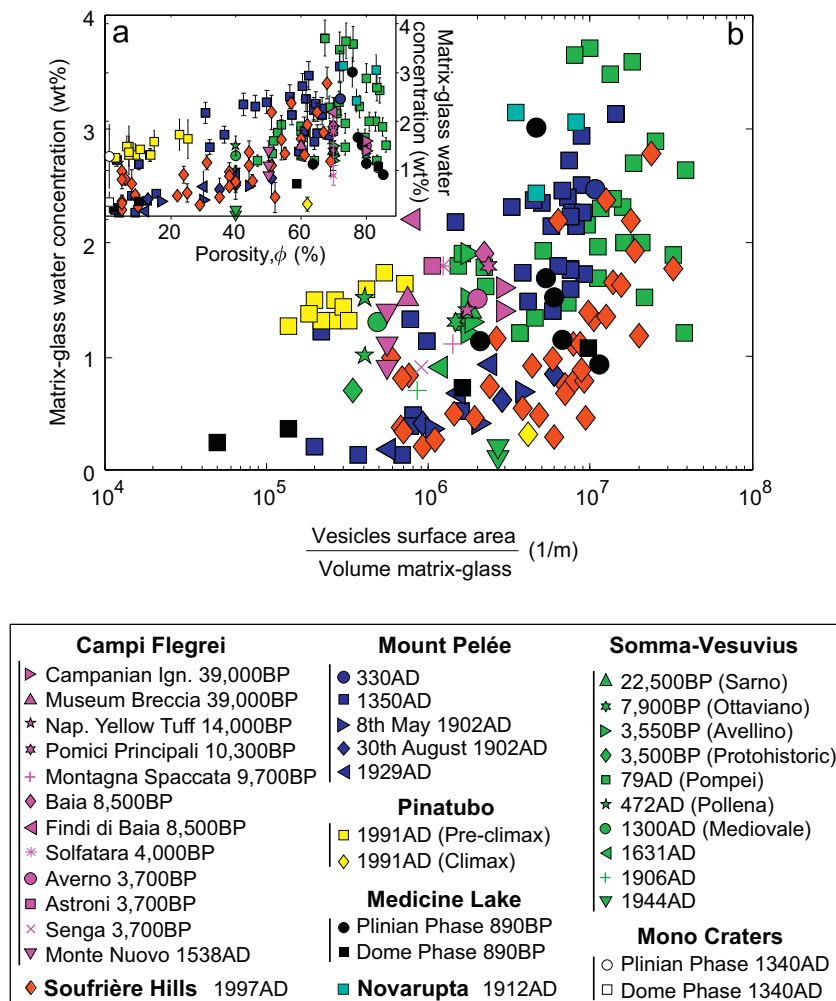


Fig. 1. (a) Matrix-glass water concentration,  $C_s$ , as a function of bulk porosity,  $\phi$ . (b) Matrix-glass water concentration, as a function of specific surface area, the ratio of vesicles surface area ( $N_v \times 4\pi R^2$ ) over the volume of glass, defined as  $(1-\phi) \times (1-x) \times (1-m)$ , with  $x$  being the volume of phenocrysts per volume of solid and  $m$  the volume of microlites per volume of groundmass. All the data and sources are summarized in Table 1.

**Table 1**

Textural and chemical parameters of samples from explosive eruptions: volume of vesicles per volume of pyroclast,  $\phi$ , volume of phenocrysts per volume of solid (i.e., phenocrysts+microlites+glass),  $x$ , volume of microlites per volume of groundmass (i.e., glass+microlites),  $m$ , vesicle number density per volume of solid,  $N_v$ , matrix-glass water content,  $C_s$ , and groundmass water content,  $C_{s-gr}$ . Either  $C_s$  or  $C_{s-gr}$  is calculated depending on the data provided, using  $C_{s-gr} \approx C_s \times (1-m)$ , assuming the equivalence of volume percentage to weight percentage. The time between sample eruption and analysis,  $\tau$ , is calculated by subtracting eruption date to the date of first submission of the corresponding paper or to the date of sample analysis when known. Water is measured either manometrically (Newman et al., 1988), by ion probe (Gerlach et al., 1996; Martel and Poussineau, 2007), FTIR (Hammer et al., 1999; Mastrolorenzo and Pappalardo, 2006), "by difference" method using electron microprobe (Balcone-Boissard et al., 2008; Martel and Poussineau, 2007), KFT (Burgisser et al., 2010), IAG or TGA (this study, cf. Appendix A). In Villemant and Boudon (1999),  $C_{s-gr}$  is calculated by correcting the bulk rock water contents for phenocryst content.  $\phi$  is measured either by image-analysis (Burgisser et al., 2010), pycnometry (Mastrolorenzo and Pappalardo, 2006; this study), or Archimedes' principle (Adams et al., 2006; Balcone-Boissard et al., 2008; Hammer et al., 1999; Martel and Poussineau, 2007; Martel et al., 2000; Villemant and Boudon, 1999). For Mono Craters (Newman et al., 1988)  $\phi$  is taken equal to 1% on the basis of samples description.  $x$  is calculated either by mass balance (Balcone-Boissard et al., 2008; Villemant and Boudon, 1999), image analysis (Adams et al., 2006; Mastrolorenzo and Pappalardo, 2006; Burgisser et al., 2010), taken from literature (Newman et al., 1988; Hammer et al., 1999; Martel and Poussineau, 2007; this study).  $m$  is obtained by image analysis (Hammer et al., 1999; Adams et al., 2006; Martel and Poussineau, 2007; Burgisser et al., 2010), mass balance calculation (Balcone-Boissard et al., 2008) or from literature (Newman et al., 1988; Villemant and Boudon, 1999; this study).  $N_v$  taken from literature for Soufrière Hills 1997 (Giachetti et al., 2010), Somma-Vesuvius (Gurioli et al., 2005; Mastrolorenzo and Pappalardo, 2006), Pinatubo 1991 (Polacci et al., 2001), Novarupta 1912 (Adams et al., 2006), Campi Flegrei (Mastrolorenzo and Pappalardo, 2006), and Mono Crater (Heiken and Wohletz, 1987). For Mount Pelée and Medicine Lake, we assumed that  $N_v$  is comprised in the range given by the other rhyolitic eruptions ( $0.26-6.7 \times 10^{15} \text{ m}^{-3}$ ), because of the apparent textural similarity of the clasts of these eruptions at a given porosity.  $N$  is then calculated using  $N=N_v \times (1-x) \times (1-m)$ .  $S$  and  $R$  were calculated using Eqs. (1) and (2), respectively. t-phonolite=tephri-phonolite, p-tephrite=phonolite-tephrite.

Volcano (reference)	Eruption type and date/age	$\tau$ (yr)	Magma chemistry	Type of deposit	$\log N_v$ ( $\text{m}^{-3}$ )	$\log N$ ( $\text{m}^{-3}$ )	$C_s$ (wt%)	$C_{s-gr}$ (wt%)	$\phi$	$x$	$m$	$R$ ( $\mu\text{m}$ )	$S$ ( $\mu\text{m}$ )	
Mount Pelée (Villemant and Boudon, 1999)	Plinian, 1350 AD (P1)	648	Andesite	Vulcanian fallout	$15.1 \pm 0.7^a$	$14.6 \pm 0.7$	$2.51 \pm 0.25$	$1.88 \pm 0.25$	0.565	0.55	$0.25^b$	10.02	11.02	
					$14.6 \pm 0.7$	$2.40 \pm 0.24$	$1.80 \pm 0.24$	0.495	0.58	$0.25^b$	9.55	10.47		
					$14.6 \pm 0.7$	$2.35 \pm 0.23$	$1.76 \pm 0.23$	0.424	0.57	$0.25^b$	8.61	9.71		
					$14.7 \pm 0.7$	$0.13 \pm 0.01$	$0.10 \pm 0.01$	0.091	0.52	$0.25^b$	4.26	7.08		
		$14.7 \pm 0.7$	$0.13 \pm 0.02$	$0.10 \pm 0.02$	0.042	0.52	$0.25^b$	3.22	6.77					
		Dome	$15.1 \pm 0.7^a$	$14.5 \pm 0.7$	$1.48 \pm 0.15$	$0.89 \pm 0.15$	0.319	0.55	$0.40^b$	7.83	9.12			
			$14.6 \pm 0.7$	$1.13 \pm 0.11$	$0.68 \pm 0.11$	0.102	0.49	$0.40^b$	4.67	7.24				
			$14.6 \pm 0.7$	$1.73 \pm 0.17$	$1.04 \pm 0.17$	0.364	0.47	$0.40^b$	7.92	9.18				
			$14.6 \pm 0.7$	$0.48 \pm 0.05$	$0.29 \pm 0.05$	0.081	0.49	$0.40^b$	4.29	7.09				
		$14.6 \pm 0.7$	$0.52 \pm 0.05$	$0.31 \pm 0.05$	0.156	0.51	$0.40^b$	5.60	7.68					
		Plinian fallout	$15.1 \pm 0.7^a$	$14.8 \pm 0.7$	$1.72 \pm 0.17$	$1.55 \pm 0.17$	0.687	0.45	$0.10^b$	10.71	11.47			
				$14.8 \pm 0.7$	$1.59 \pm 0.16$	$1.43 \pm 0.16$	0.641	0.48	$0.10^b$	10.15	10.98			
	$14.8 \pm 0.7$			$1.76 \pm 0.18$	$1.58 \pm 0.18$	0.649	0.46	$0.10^b$	10.20	11.02				
	$14.8 \pm 0.7$			$2.14 \pm 0.21$	$1.93 \pm 0.21$	0.664	0.46	$0.10^b$	10.37	11.17				
	$14.8 \pm 0.7$			$2.26 \pm 0.23$	$2.03 \pm 0.23$	0.639	0.48	$0.10^b$	10.18	11.00				
	$14.8 \pm 0.7$			$2.27 \pm 0.23$	$2.04 \pm 0.23$	0.664	0.49	$0.10^b$	10.58	11.34				
	$14.8 \pm 0.7$			$2.23 \pm 0.22$	$2.01 \pm 0.22$	0.639	0.48	$0.10^b$	10.14	10.97				
	$14.8 \pm 0.7$			$2.46 \pm 0.25$	$2.21 \pm 0.25$	0.616	0.48	$0.10^b$	9.83	10.70				
	$14.7 \pm 0.7$			$2.94 \pm 0.29$	$2.65 \pm 0.29$	0.623	0.55	$0.10^b$	10.40	11.19				
	$14.8 \pm 0.7$			$1.39 \pm 0.14$	$1.25 \pm 0.14$	0.593	0.48	$0.10^b$	9.52	10.44				
	$14.9 \pm 0.7$			$2.37 \pm 0.24$	$2.13 \pm 0.24$	0.645	0.27	$0.10^b$	9.16	10.15				
	$14.7 \pm 0.7$			$3.13 \pm 0.31$	$2.82 \pm 0.31$	0.719	0.52	$0.10^b$	11.80	12.43				
	$14.7 \pm 0.7$			$2.72 \pm 0.27$	$2.45 \pm 0.27$	0.605	0.53	$0.10^b$	10.01	10.86				
	$14.7 \pm 0.7$			$2.14 \pm 0.21$	$1.93 \pm 0.21$	0.571	0.51	$0.10^b$	9.41	10.35				
	$14.8 \pm 0.7$			$2.31 \pm 0.23$	$2.08 \pm 0.23$	0.459	0.50	$0.10^b$	8.03	9.26				
	$14.8 \pm 0.7$			$2.18 \pm 0.22$	$1.96 \pm 0.22$	0.306	0.46	$0.10^b$	6.32	8.09				
	$14.7 \pm 0.7$			$1.32 \pm 0.13$	$1.19 \pm 0.13$	0.136	0.54	$0.10^b$	4.72	7.25				
	$14.7 \pm 0.7$			$0.38 \pm 0.04$	$0.34 \pm 0.04$	0.128	0.56	$0.10^b$	4.67	7.24				
	$14.8 \pm 0.7$	$1.21 \pm 0.12$	$1.09 \pm 0.12$	0.034	0.49	$0.10^b$	2.78	6.68						
	$14.8 \pm 0.7$	$0.20 \pm 0.02$	$0.18 \pm 0.02$	0.029	0.50	$0.10^b$	2.64	6.66						
	Mount Pelée (Martel and Poussineau, 2007)	Dome, 1929 AD	78	Andesite	Block and ash flow	$15.1 \pm 0.7^a$	$14.8 \pm 0.7$	$0.17 \pm 0.01$	$0.15 \pm 0.01$	0.120	0.47	0.12	4.33	7.10
						$14.8 \pm 0.7$	$0.67 \pm 0.32$	$0.59 \pm 0.32$	0.300	0.47	0.12	6.34	8.10	
		Dome, 1902 AD May 8th	105	Andesite	Surge	$15.1 \pm 0.7^a$	$14.7 \pm 0.7$	$0.93 \pm 0.05$	$0.82 \pm 0.05$	0.400	0.47	0.12	7.34	8.76
						$14.7 \pm 0.7$	$0.36 \pm 0.05$	$0.27 \pm 0.05$	0.170	0.47	0.26	5.52	7.50	
						$14.7 \pm 0.7$	$0.40 \pm 0.06$	$0.30 \pm 0.06$	0.300	0.47	0.26	6.71	8.34	
		Dome, 1902 AD Aug 30th	105	Andesite	Surge	$14.7 \pm 0.7$	$0.68 \pm 0.05$	$0.50 \pm 0.05$	0.440	0.47	0.26	8.22	9.41	
$15.1 \pm 0.7^a$						$14.7 \pm 0.7$	$0.41 \pm 0.05$	$0.28 \pm 0.05$	0.130	0.47	0.31	4.84	7.31	

Table 1 (continued)

Volcano (reference)	Eruption type and date/age	$\tau$ (yr)	Magma chemistry	Type of deposit	$\log N_v$ ( $m^{-3}$ )	$\log N$ ( $m^{-3}$ )	$C_s$ (wt%)	$C_{s-gr}$ (wt%)	$\phi$	$x$	$m$	$R$ ( $\mu m$ )	$S$ ( $\mu m$ )
						14.7 ± 0.7	0.61 ± 0.23	0.42 ± 0.23	0.350	0.47	0.31	7.42	8.81
						14.7 ± 0.7	0.84 ± 0.33	0.58 ± 0.33	0.510	0.47	0.31	9.24	10.21
	Plinian, 1350 AD (P1)	657	Andesite	Fallout	15.1 ± 0.7 <sup>a</sup>	14.8 ± 0.7	1.80 ± 0.30	1.61 ± 0.30	0.610	0.47	0.11	9.72	10.61
	Plinian, 330 AD (P2)	1677	Andesite	Fallout	15.1 ± 0.7 <sup>a</sup>	14.8 ± 0.7	2.47 ± 0.33	2.40 ± 0.33	0.720	0.47	0.03	11.15	11.85
Neapolitan volcanoes (Mastrolorenzo and Pappalardo, 2006)	Strombolian, 1538 AD (Monte Nuovo)	467	Trachyte	Scoria	13.4 ± 0.3 <sup>c</sup>	13.2 ± 0.3	1.10 ± 0.20	1.10 ± 0.20	0.500	0.03 <sup>d</sup>	0.32	25.56	30.27
						13.2 ± 0.3	1.40 ± 0.20	1.40 ± 0.20	0.500	0.03 <sup>d</sup>	0.32	25.56	30.27
						13.2 ± 0.3	0.90 ± 0.02	0.90 ± 0.02	0.500	0.03 <sup>d</sup>	0.32	25.56	30.27
	Strombolian, 3.7 ka BP (Senga)	3700	Andesite	Scoria	13.4 ± 0.3 <sup>c</sup>	13.4 ± 0.3	0.90 ± 0.02	0.90 ± 0.02	0.700	0.05 <sup>e</sup>	0.00	29.12	32.63
	Strombolian, 3.7 ka BP (Averno)	3700	Trachyte	Pumice	13.4 ± 0.3 <sup>c</sup>	13.4 ± 0.3	1.50 ± 0.10	1.50 ± 0.10	0.800	0.07	0.00	35.43	37.97
	Strombolian, 3.7 ka BP (Astroni)	3700	Trachyte	Pumice	13.6 ± 0.4 <sup>c</sup>	13.6 ± 0.4	1.80 ± 0.30	1.80 ± 0.30	0.700	0.06 <sup>f</sup>	0.00	25.45	28.49
	Strombolian, 4 ka BP (Solfatara)	4000	Trachyte	Pumice	13.8 ± 0.3 <sup>c</sup>	13.8 ± 0.3	1.80 ± 0.30	1.80 ± 0.30	0.700	0.05 <sup>e</sup>	0.00	21.42	24.00
	Strombolian, 8.5 ka BP (Fondi di Baia)	8500	Trachyte	Pumice	13.3 ± 0.3 <sup>c</sup>	13.3 ± 0.3	2.20 ± 0.30	2.20 ± 0.30	0.700	0.05 <sup>e</sup>	0.00	32.67	36.61
	Strombolian, 8.5 ka BP (Baia)	8500	Trachyte	Pumice	14.5 ± 0.3 <sup>c</sup>	14.5 ± 0.3	1.90 ± 0.30	1.90 ± 0.30	0.700	0.05 <sup>e</sup>	0.05	13.23	14.75
	Strombolian, 9.7 ka BP (Montagna Spaccata)	9700	Trachyte	Pumice	14.0 ± 0.3 <sup>c</sup>	14.0 ± 0.3	1.10 ± 0.40	1.10 ± 0.40	0.700	0.05 <sup>e</sup>	0.00	18.80	21.07
	Plinian, 10.3 ka BP (Pomici Principali)	10,300	Trachyte	Pumice	14.6 ± 0.3 <sup>c</sup>	14.6 ± 0.3	1.80 ± 0.10	1.80 ± 0.10	0.700	0.07	0.00	11.78	13.17
	Plinian, 14 ka BP (Yellow Tuff)	14,000	Trachyte	Pumice	14.3 ± 0.3 <sup>c</sup>	14.3 ± 0.3	1.40 ± 0.10	1.40 ± 0.10	0.700	0.03 <sup>g</sup>	0.00	14.49	16.27
	Plinian, 39 ka BP (Museum Breccia)	39,000	Trachyte	Pumice	13.6 ± 0.3 <sup>c</sup>	13.5 ± 0.3	1.50 ± 0.10	1.50 ± 0.10	0.600	0.16 <sup>h</sup>	0.00	22.32	25.87
	Plinian, 39 ka BP (Campanian Ignimbrite)	39,000	Trachyte	Tuff	14.0 ± 0.3 <sup>c</sup>	14.0 ± 0.3	1.40 ± 0.10	1.40 ± 0.10	0.800	0.03 <sup>i</sup>	0.00	22.34	24.02
						14.0 ± 0.3	1.60 ± 0.08	1.60 ± 0.08	0.800	0.03 <sup>i</sup>	0.00	22.34	24.02
Pinatubo (Hammer et al., 1999)	Plinian, 1991 AD (pre-climax)	6	Dacite	Surge	14.8 ± 0.3 <sup>j</sup>	14.5 ± 0.3	1.49 ± 0.41	1.26 ± 0.41	0.071	0.40 <sup>k</sup>	0.2	4.20	8.14
						14.5 ± 0.3	1.31 ± 0.23	1.13 ± 0.23	0.090	0.40 <sup>k</sup>	0.1	4.40	8.20
						14.6 ± 0.3	1.73 ± 0.32	1.66 ± 0.32	0.226	0.40 <sup>k</sup>	0.0	6.10	8.85
						14.5 ± 0.3	1.31 ± 0.40	1.20 ± 0.40	0.071	0.40 <sup>k</sup>	0.1	4.04	8.10
						14.5 ± 0.3	1.49 ± 0.22	1.27 ± 0.22	0.064	0.40 <sup>k</sup>	0.1	3.89	8.07
						14.5 ± 0.3	1.64 ± 0.40	1.48 ± 0.40	0.252	0.40 <sup>k</sup>	0.1	6.62	9.11
						14.5 ± 0.3	1.43 ± 0.06	1.28 ± 0.06	0.105	0.40 <sup>k</sup>	0.1	4.66	8.28
						14.5 ± 0.3	1.59 ± 0.23	1.51 ± 0.23	0.150	0.40 <sup>k</sup>	0.1	5.34	8.52
						14.6 ± 0.3	1.37 ± 0.12	1.35 ± 0.12	0.071	0.40 <sup>k</sup>	0.0	3.90	8.07
						14.5 ± 0.3	1.26 ± 0.06	0.99 ± 0.06	0.030	0.40 <sup>k</sup>	0.2	3.11	7.91
						14.6 ± 0.3	1.31 ± 0.12	1.30 ± 0.12	0.139	0.40 <sup>k</sup>	0.0	5.00	8.39
Pinatubo (Gerlach et al., 1996)	Plinian, 1991 AD (climax)	0.5	Dacite	Pyroclastic flow	14.8 ± 0.3 <sup>j</sup>	14.5 ± 0.3	0.31 ± 0.15	0.28 ± 0.15	0.620 <sup>l</sup>	0.45	0.1 <sup>m</sup>	11.26	12.37
Soufrière Hills (Burgisser et al., 2010)	Vulcanian, 1997 AD	10	Andesite	Dense sample (degassed plug)	15.4 ± 0.4 <sup>n</sup>	14.9 ± 0.4	0.37 ± 0.13	0.23 ± 0.13	0.050	0.49	0.39	2.65	5.05
						14.8 ± 0.4	0.20 ± 0.07	0.10 ± 0.07	0.050	0.47	0.51	2.81	5.09
						14.9 ± 0.4	0.26 ± 0.06	0.14 ± 0.06	0.100	0.40	0.46	3.35	5.28
				Homogeneous pumices from pyroclastic flows	15.4 ± 0.4 <sup>n</sup>	15.0 ± 0.4	1.18 ± 0.30	0.86 ± 0.30	0.690	0.51	0.27	8.81	9.26
						14.9 ± 0.4	0.45 ± 0.31	0.31 ± 0.31	0.520	0.53	0.31	7.16	7.81
						14.8 ± 0.4	0.74 ± 0.33	0.50 ± 0.33	0.400	0.59	0.32	6.41	7.20
						14.8 ± 0.4	0.77 ± 0.21	0.49 ± 0.21	0.400	0.59	0.36	6.54	7.30
						15.0 ± 0.4	2.19 ± 0.35	2.19 ± 0.35	0.510	0.60	0.00	6.59	7.34
						15.1 ± 0.4	0.45 ± 0.04	0.45 ± 0.04	0.350	0.47	0.00	4.82	6.05
						14.8 ± 0.4	0.54 ± 0.19	0.35 ± 0.19	0.250	0.59	0.35	5.16	6.28
						15.0 ± 0.4	1.32 ± 0.14	0.83 ± 0.14	0.610	0.37	0.37	7.57	8.16
				Homogeneous pumices from fallout	15.4 ± 0.4 <sup>n</sup>	14.9 ± 0.4	1.35 ± 0.12	1.09 ± 0.12	0.550	0.63	0.19	7.65	8.23
						14.9 ± 0.4	2.19 ± 0.19	1.93 ± 0.19	0.650	0.62	0.12	8.48	8.96
						14.9 ± 0.4	1.93 ± 0.61	1.56 ± 0.61	0.620	0.64	0.19	8.50	8.98
						14.9 ± 0.4	1.65 ± 0.17	1.42 ± 0.17	0.600	0.62	0.14	7.96	8.50
						14.9 ± 0.4	2.79 ± 0.33	2.48 ± 0.33	0.680	0.65	0.11	9.08	9.51

						14.9 ± 0.4	2.38 ± 0.12	2.09 ± 0.12	0.570	0.64	0.12	7.72	8.29
						14.8 ± 0.4	1.77 ± 0.12	1.47 ± 0.12	0.670	0.70	0.17	9.64	10.02
			Breadcrust bomb		15.4 ± 0.4 <sup>n</sup>	14.9 ± 0.4	1.10 ± 0.34	0.80 ± 0.34	0.440	0.60	0.27	6.66	7.40
						14.9 ± 0.4	0.83 ± 0.13	0.57 ± 0.13	0.060	0.54	0.31	2.81	5.09
						15.0 ± 0.4	1.16 ± 0.15	0.79 ± 0.15	0.310	0.42	0.32	5.00	6.17
						14.9 ± 0.4	0.99 ± 0.19	0.63 ± 0.19	0.050	0.47	0.36	2.57	5.03
						14.8 ± 0.4	1.63 ± 0.41	1.06 ± 0.41	0.540	0.61	0.35	7.98	8.52
			Heterogeneous pumices		15.4 ± 0.4 <sup>n</sup>	14.9 ± 0.4	0.81 ± 0.18	0.51 ± 0.18	0.050	0.51	0.37	2.66	5.05
						14.8 ± 0.4	0.49 ± 0.09	0.33 ± 0.09	0.090	0.61	0.33	3.46	5.33
						14.8 ± 0.4	0.78 ± 0.14	0.51 ± 0.14	0.450	0.58	0.35	6.91	7.60
						14.7 ± 0.4	0.73 ± 0.29	0.51 ± 0.29	0.080	0.74	0.30	3.74	5.46
						14.9 ± 0.4	0.97 ± 0.19	0.68 ± 0.19	0.380	0.58	0.30	6.12	6.97
						14.8 ± 0.4	0.29 ± 0.08	0.17 ± 0.08	0.290	0.60	0.43	5.82	6.74
						14.8 ± 0.4	0.88 ± 0.09	0.54 ± 0.09	0.380	0.62	0.39	6.62	7.37
						14.7 ± 0.4	0.48 ± 0.06	0.32 ± 0.06	0.220	0.68	0.34	5.28	6.36
						14.8 ± 0.4	1.38 ± 0.22	1.01 ± 0.22	0.440	0.65	0.27	6.97	7.65
						14.9 ± 0.4	0.33 ± 0.04	0.19 ± 0.04	0.050	0.48	0.41	2.66	5.05
						14.8 ± 0.4	0.67 ± 0.08	0.42 ± 0.08	0.380	0.57	0.38	6.32	7.13
						14.8 ± 0.4	0.91 ± 0.17	0.60 ± 0.17	0.240	0.64	0.34	5.27	6.35
						14.9 ± 0.4	1.10 ± 0.10	0.85 ± 0.10	0.510	0.57	0.23	7.02	7.69
Medicine Lake, Glass Mountain (this study)	Plinian, 1110 AD	902	Rhyolitic	Fallout	15.1 ± 0.7 <sup>a</sup>	15.1 ± 0.7	1.52 ± 0.15	1.52 ± 0.15	0.787	0.00 <sup>o</sup>	0.00 <sup>o</sup>	10.08	10.92
						15.1 ± 0.7	1.14 ± 0.11	1.14 ± 0.11	0.800	0.00 <sup>o</sup>	0.00 <sup>o</sup>	10.35	11.15
						15.1 ± 0.7	1.13 ± 0.11	1.13 ± 0.11	0.636	0.00 <sup>o</sup>	0.00 <sup>o</sup>	7.85	9.13
						15.1 ± 0.7	3.01 ± 0.30	3.01 ± 0.30	0.758	0.00 <sup>o</sup>	0.00 <sup>o</sup>	9.54	10.46
						15.1 ± 0.7	1.68 ± 0.17	1.68 ± 0.17	0.774	0.00 <sup>o</sup>	0.00 <sup>o</sup>	9.83	10.70
						15.1 ± 0.7	0.92 ± 0.09	0.92 ± 0.09	0.852	0.00 <sup>o</sup>	0.00 <sup>o</sup>	11.68	12.32
	Dome, 1110 AD		Obsidians (vesicular parts)		15.1 ± 0.7 <sup>a</sup>	15.1 ± 0.7	0.72 ± 0.07	0.72 ± 0.07	0.587	0.00 <sup>o</sup>	0.00 <sup>o</sup>	7.33	8.75
			Obsidians (dense parts)		15.1 ± 0.7 <sup>a</sup>	15.1 ± 0.7	1.07 ± 0.11	1.07 ± 0.11	0.837	0.00 <sup>o</sup>	0.00 <sup>o</sup>	11.25	11.93
						15.1 ± 0.7	0.24 ± 0.02	0.24 ± 0.02	0.027	0.00 <sup>o</sup>	0.00 <sup>o</sup>	1.97	6.58
						15.1 ± 0.7	0.36 ± 0.04	0.36 ± 0.04	0.101	0.00 <sup>o</sup>	0.00 <sup>o</sup>	3.15	6.75
Somma–Vesuvius (Balcone-Boissard et al., 2008)	Plinian, 79 AD (Pompei)	1928	Phonolitic	Fallout	14.8 ± 0.7 <sup>p</sup>	14.6 ± 0.7	1.47 ± 0.15	0.94 ± 0.15	0.735	0.06	0.36 <sup>q</sup>	12.25	13.08
						14.6 ± 0.7	1.78 ± 0.18	1.14 ± 0.18	0.528	0.06	0.36 <sup>q</sup>	9.05	10.45
						14.6 ± 0.7	2.00 ± 0.20	1.28 ± 0.20	0.829	0.06	0.36 <sup>q</sup>	14.76	15.35
						14.6 ± 0.7	1.68 ± 0.17	1.13 ± 0.17	0.797	0.06	0.33 <sup>q</sup>	13.58	14.26
						14.6 ± 0.7	1.20 ± 0.12	0.81 ± 0.12	0.640	0.06	0.33 <sup>q</sup>	10.42	11.53
						14.6 ± 0.7	1.52 ± 0.15	1.02 ± 0.15	0.860	0.06	0.33 <sup>q</sup>	15.76	16.28
						14.5 ± 0.7	2.00 ± 0.20	1.04 ± 0.20	0.810	0.11	0.48 <sup>q</sup>	15.46	16.00
						14.5 ± 0.7	1.96 ± 0.20	1.02 ± 0.20	0.735	0.11	0.48 <sup>q</sup>	13.39	14.10
						14.5 ± 0.7	2.31 ± 0.23	1.20 ± 0.23	0.780	0.11	0.48 <sup>q</sup>	14.54	15.14
						14.5 ± 0.7	2.16 ± 0.22	1.12 ± 0.22	0.710	0.11	0.48 <sup>q</sup>	12.85	13.61
						14.5 ± 0.7	1.89 ± 0.19	0.98 ± 0.19	0.851	0.11	0.48 <sup>q</sup>	17.04	17.49
						14.4 ± 0.7	3.59 ± 0.36	1.54 ± 0.36	0.759	0.10	0.57 <sup>q</sup>	14.82	15.40
						14.4 ± 0.7	2.89 ± 0.29	1.24 ± 0.29	0.800	0.10	0.57 <sup>q</sup>	16.04	16.55
						14.4 ± 0.7	3.48 ± 0.35	1.49 ± 0.35	0.718	0.10	0.57 <sup>q</sup>	13.80	14.47
						14.4 ± 0.7	3.71 ± 0.37	1.59 ± 0.37	0.673	0.10	0.57 <sup>q</sup>	12.86	13.62
						14.4 ± 0.7	2.64 ± 0.26	1.13 ± 0.26	0.842	0.10	0.57 <sup>q</sup>	17.66	18.07
						14.4 ± 0.7	2.30 ± 0.23	1.01 ± 0.23	0.687	0.15	0.56 <sup>f</sup>	13.28	13.99
						14.4 ± 0.7	1.77 ± 0.18	0.78 ± 0.18	0.615	0.15	0.56 <sup>f</sup>	11.94	12.81
						14.4 ± 0.7	1.93 ± 0.19	0.85 ± 0.19	0.540	0.15	0.56 <sup>f</sup>	10.78	11.82
						14.4 ± 0.7	1.20 ± 0.12	0.53 ± 0.12	0.466	0.15	0.56 <sup>f</sup>	9.76	11.00
						14.4 ± 0.7	1.34 ± 0.13	0.59 ± 0.13	0.512	0.15	0.56 <sup>f</sup>	10.38	11.49
						14.4 ± 0.7	1.20 ± 0.12	0.53 ± 0.12	0.834	0.15	0.56 <sup>f</sup>	17.50	17.92
						14.4 ± 0.7	2.39 ± 0.24	1.05 ± 0.24	0.716	0.15	0.56 <sup>f</sup>	13.90	14.56
						14.6 ± 0.7	3.65 ± 0.37	2.41 ± 0.37	0.739	0.13	0.34 <sup>f</sup>	12.54	13.33
						14.6 ± 0.7	1.61 ± 0.16	1.06 ± 0.16	0.516	0.13	0.34 <sup>f</sup>	9.05	10.45
						14.6 ± 0.7	2.70 ± 0.27	1.78 ± 0.27	0.833	0.13	0.34 <sup>f</sup>	15.14	15.70
Somma–Vesuvius (Mastrolorenzo and Pappalardo, 2006)	Strombolian, 1944 AD	61	p-Tephrite	Scoria	14.9 ± 0.3	14.5 ± 0.3	0.10 ± 0.01	0.10 ± 0.01	0.400	0.60 <sup>s</sup>	0.02	8.21	9.58
	Sub-plinian, 1906 AD	99	p-Tephrite	Pumice	13.9 ± 0.3	13.6 ± 0.3	0.70 ± 0.03	0.70 ± 0.03	0.400	0.50 <sup>s</sup>	0.01	16.36	19.69

Table 1 (continued)

Volcano (reference)	Eruption type and date/age	$\tau$ (yr)	Magma chemistry	Type of deposit	$\log N_v$ ( $m^{-3}$ )	$\log N$ ( $m^{-3}$ )	$C_s$ (wt%)	$C_{s-gr}$ (wt%)	$\phi$	$x$	$m$	$R$ ( $\mu m$ )	$S$ ( $\mu m$ )
	Sub-plinian, 1631 AD	374	t-Phonolite	Pumice	14.3 ± 0.3	14.0 ± 0.3	0.90 ± 0.08	0.90 ± 0.08	0.400	0.50 <sup>f</sup>	0.02	11.89	14.29
	Strombolian, 1300 AD (Medioevale)	705	t-Phonolite	Scoria	13.2 ± 0.3	12.9 ± 0.3	1.30 ± 0.10	1.30 ± 0.10	0.400	0.50 <sup>f</sup>	0.00	27.91	33.63
	Plinian, 472 AD (Pollena)	1533	p-tephrite	Scoria	14.0 ± 0.3	13.9 ± 0.3	1.00 ± 0.10	1.00 ± 0.10	0.400	0.18 <sup>u</sup>	0.02	13.12	17.06
			t-Phonolite	Pumice	14.0 ± 0.3	13.9 ± 0.3	1.50 ± 0.20	1.50 ± 0.20	0.400	0.18 <sup>u</sup>	0.02	13.12	17.06
	Plinian, 79 AD (Pompei)	1926	t-Phonolite	Pumice	14.8 ± 0.7	14.8 ± 0.7	1.80 ± 0.03	1.76 ± 0.03	0.600	0.05 <sup>v</sup>	0.02	8.64	10.15
						14.8 ± 0.7	1.90 ± 0.06	1.86 ± 0.06	0.600	0.08 <sup>v</sup>	0.02	8.73	10.21
						14.8 ± 0.7	1.30 ± 0.10	1.27 ± 0.10	0.600	0.08 <sup>v</sup>	0.02	8.73	10.21
	Sub-plinian, 3.5 ka BP (Protohistoric)	3500	t-Phonolite	Pumice	12.7 ± 0.3	12.4 ± 0.3	0.70 ± 0.01	0.70 ± 0.01	0.400	0.50 <sup>f</sup>	0.03	42.34	50.81
	Plinian, 3.55 ka (Avellino)	3550	Phonolite	Pumice	14.0 ± 0.3	13.9 ± 0.3	1.30 ± 0.10	1.27 ± 0.10	0.700	0.15 <sup>v</sup>	0.02	19.81	21.92
						13.9 ± 0.3	1.20 ± 0.10	1.18 ± 0.10	0.700	0.15 <sup>v</sup>	0.02	19.81	21.92
						13.9 ± 0.3	1.50 ± 0.50	1.47 ± 0.50	0.700	0.15 <sup>v</sup>	0.02	19.81	21.92
						13.9 ± 0.3	1.90 ± 0.30	1.86 ± 0.30	0.700	0.15 <sup>v</sup>	0.02	19.81	21.92
			t-Phonolite	Pumice	14.0 ± 0.3	13.9 ± 0.3	1.30 ± 0.30	1.27 ± 0.30	0.700	0.18 <sup>v</sup>	0.02	20.02	22.10
	Plinian, 7.9 ka BP (Ottaviano)	7900	Trachyte	Pumice	13.0 ± 0.3	13.0 ± 0.3	1.30 ± 0.05	1.29 ± 0.05	0.800	0.05 <sup>w</sup>	0.01	47.16	50.60
	Plinian, 22.5 ka BP (Sarno)	22,500	Trachyte	Pumice	14.2 ± 0.3	14.2 ± 0.3	1.40 ± 0.03	1.40 ± 0.03	0.700	0.10 <sup>x</sup>	0.00	16.17	18.02
Novarupta (this study)	Plinian, 1912 AD	100	Dacite	Pumice	14.9 ± 0.4 <sup>y</sup>	14.9 ± 0.4	2.43 ± 0.24	2.43 ± 0.24	0.770	0.05 <sup>y</sup>	0.00 <sup>y</sup>	12.07	13.11
						14.9 ± 0.4	3.06 ± 0.31	3.06 ± 0.31	0.830	0.05 <sup>y</sup>	0.00 <sup>y</sup>	13.68	14.52
						14.9 ± 0.4	3.15 ± 0.32	3.15 ± 0.32	0.730	0.05 <sup>y</sup>	0.00 <sup>y</sup>	11.24	12.42
Mono Craters (Newman et al., 1988)	Plinian, 1340 AD	648	Rhyolitic	Obsidian clasts in tephra	13 <sup>z</sup>	13 <sup>z</sup>	1.29 ± 0.69	1.29 ± 0.69	0.010	0.00	0.00	6.22	288.91
	Domes, 1340 AD	648	Rhyolitic	Dome deposits	13 <sup>z</sup>	13 <sup>z</sup>	0.35 ± 0.22	0.35 ± 0.22	0.010	0.00	0.00	6.22	288.91

<sup>a</sup> Estimated to be in the ranges given by the other rhyolitic eruptions of Pinatubo and Soufrière Hills.

<sup>b</sup> Data calculated using the average of the ranges given in Table 2 of Martel et al. (2000). For Vulcanian clasts,  $m$  was considered to be in between that of the Plinian pumices and the dome sample. This value (0.25) is similar to the average microlite volume fraction of the 1997 Vulcanian samples of Soufrière Hills (0.29; Burgisser et al., 2010).

<sup>c</sup> Error estimated to be 20% of  $\log N_v$ .

<sup>d</sup> From D'Oriano et al. (2005).

<sup>e</sup> Average of the phenocryst contents of samples from the other Neapolitan volcanoes eruptions.

<sup>f</sup> From Isia et al. (2004).

<sup>g</sup> From Wohletz et al. (1995).

<sup>h</sup> From Fuglignati et al. (2004).

<sup>i</sup> From Civetta et al. (1997).

<sup>j</sup> From Polacci et al. (2001). The vesicle number density was estimated to be the same for both the pre-climax and the climax phases.

<sup>k</sup> Phenocryst content close to that of the crystal-rich climactic material (Hammer, J., personal communication). Data from Pallister et al. (1996).

<sup>l</sup> Porosity of phenocryst-rich dacite is 63% according to Bernard et al. (1996) and 61% according to Pallister et al. (1996).

<sup>m</sup> Supposed to be as low as in the similar samples of Hammer et al. (1999).

<sup>n</sup> From Giachetti et al. (2010).

<sup>o</sup> From Heiken (1978).

<sup>p</sup> Considered to be in the range given by Mastrolorenzo and Pappalardo (2006) ( $\log N_v = 14.08$ ) and that of Gurioli et al. (2005) (14.15–15.54).

<sup>q</sup> From Gurioli et al. (2005).

<sup>r</sup> From Balcone-Boissard et al. (2011).

<sup>s</sup> From Villemant et al. (1993).

<sup>t</sup> Considered to be similar to that of the other Vesuvius Strombolian and sub-plinian samples.

<sup>u</sup> From Rosi and Santacrose (1983).

<sup>v</sup> From Barberi et al. (1981).

<sup>w</sup> From Bertagnini et al. (1998).

<sup>x</sup> Considered to be similar to the other Vesuvius Plinian samples, around 10%.

<sup>y</sup> From Adams et al. (2006) and Adams, N. (personal communication).

<sup>z</sup> From Heiken and Wohletz (1987).

eruption of Medicine Lake Volcano (MLV), Northern California (Donnelly-Nolan et al., 2008), and 3 new measurements of pumices from the 1912 Plinian eruption of Novarupta (Hildreth, 1983; Hildreth and Fierstein, 2012).

The MLV samples are 8 rhyolitic pumices from the Plinian phase preceding the emplacement of the Glass Mountain rhyolite flow, and 2 obsidians from the actual rhyolite flow, each of these two obsidians containing both dense and vesicular parts. The samples are aphyric with a glassy groundmass (Heiken, 1978). Dating by Nathenson et al. (2007) gives an age of 1110 AD for the MLV samples and porosity was measured by He-pycnometry following the same procedure as in Giachetti et al. (2010). Water concentration was determined by thermogravimetric analysis (TGA), following a procedure somewhat modified after Denton et al. (2009). A mass spectrometer coupled to the TGA for 2 of the 10 analyses (one obsidian and one pumice) showed that more than 95% of the volatiles exsolved during analysis are water. The porosity of the 3 Novarupta samples was taken from Adams et al. (2006) and  $C_s$  was obtained by measuring H using inert gas fusion up to 2000 °C. Details on these methods are provided in Appendix A.

Fig. 1a shows that the data range in  $\phi$  from 1% to 86% and in  $C_s$  from 0.1 wt% to 3.7 wt% with a broad positive correlation between  $\phi$  and  $C_s$  for samples from all eruptions and within individual eruptions. Relatively high vesicle interconnectivity in most of the samples, indicated by high open vs. bulk porosity ratios (0.88–0.95 in the MLV samples; 0.67–0.98 in Soufrière Hills samples; Giachetti et al., 2010), electronic microscope images (Hammer et al., 1999; Mastrolorenzo and Pappalardo, 2006; Martel and Poussineau, 2007), or vesicle size distributions (Adams et al., 2006; Giachetti et al., 2010), suggests that moisture can easily permeate a large fraction of a sample's vesicles. Consequently, it is feasible that meteoric water diffuses into the glass over much of the sample's surface area at atmospheric pressure and temperature. We refer to this post-eruptive diffusion of meteoric water into the matrix-glass of a 'cold' volcanic sample as *rehydration*. We do not include in this definition the possible hydration of the 'hot' melt/glass by interaction with a hydrothermal system or by bubble resorption. We also use the terms *secondary* water to refer to the water (meteoric) inherited from rehydration, and *primary* water to refer to the magmatic water.

### 3. Rehydration

It is known that the total matrix-glass water content of volcanic samples, especially 'old' ones, can include both primary and secondary water (e.g., Ross and Smith, 1955; Friedman and Smith, 1958, 1960; Friedman et al., 1966; Friedman and Long, 1976; Michels et al., 1983; Newman et al., 1986; Denton et al., 2009, 2012; Tuffen et al., 2010), and volcanologists need to quantify their relative amounts before interpreting magma degassing processes. Assuming sufficient availability of meteoric water (e.g., Friedman and Obradovich, 1981), rehydration is a diffusion-limited process where the degree of rehydration depends on the duration between the deposition of the sample and water analysis, as well as water solubility and diffusivity. The latter may depend on the glass chemistry, the water concentration, as well as the temperature and the relative humidity (Friedman and Long, 1976; Friedman and Obradovich, 1981; Anovitz et al., 1999, 2004, 2006, 2008; Sterpenich and Libourel, 2006; Liritzis and Laskaris, 2011). The total amount of water gained by rehydration will also depend on the specific surface area, the surface area of vesicles per unit volume of glass, a function of porosity and vesicle number density.

Thus, it is not unreasonable to assume that each sample in Fig. 1 has undergone some degree of rehydration, resulting in the

observed correlation between water concentration and porosity (Fig. 1a) or specific surface area (Fig. 1b). To conclusively discriminate between rehydration and incomplete degassing would require a substantial re-analysis of many of the analyses compiled in Fig. 1 and is unrealistic for such a large and diverse set of data. Instead, we have modeled matrix-glass rehydration to test the hypothesis that rehydration alone can explain the observed trend in Fig. 1, and to what extent the data allow for, or require, the possibility of incomplete magma degassing (e.g., Sparks, 1978; Woods and Koyaguchi, 1994; Stasiuk et al., 1996; Mangan and Sisson, 2000; Massol and Koyaguchi, 2005; Gonnermann and Manga, 2007).

## 4. Approach

### 4.1. Analytical techniques and prior work

The amount of water dissolved in the matrix-glass of a pyroclast can be directly measured using one of several bulk or punctual analytical techniques, such as for example: Karl Fisher Titration (Burgisser et al., 2010), microRaman spectrometry (Di Muro et al., 2006; Shea et al., 2012), Fourier Transform Infrared Spectroscopy (e.g., Newman et al., 1986), Synchrotron Fourier Transform Infrared Spectroscopy (e.g., Castro et al., 2012), Thermogravimetric analysis (e.g., Denton et al., 2009). Some methods can also provide constraints on whether a *texturally intact* glass has been rehydrated (Tuffen et al., 2010). They include the following: (1) the analysis of D/H isotopic ratios that differ between magmatic to meteoric water (Friedman and Smith, 1958; DeGroat-Nelson et al., 2001; Harford et al., 2003); (2) micro-analytical techniques (e.g., FTIR, nanoSIMS, microRaman) capable of resolving micron-scale water concentration gradients that decrease from the glass surface toward the glass interior and are suggestive of diffusion profiles (Anovitz et al., 2008, 2009; Watkins et al., 2012; McIntosh et al., 2013); (3) quantification of water speciation, with secondary water tending to remain as molecular water and primary water as hydroxyls, at least at low total water concentrations (Newman et al., 1988; Ihinger et al., 1994; Hammer et al., 1999; Zhang, 1999); and (4) thermogravimetric analyses, based on the assumption that secondary water is more weakly bound within the silica network than primary water (Newman et al., 1986; Roulia et al., 2006; Denton et al., 2009; Stevenson et al., 2009). However, none of these methods can be used to correct quantitatively for post-eruptive rehydration without potential problems, because important aspects of glass rehydration at very low temperatures remain unresolved (Liritzis and Laskaris, 2011 and references therein), in particular critical parameters such as water solubility and diffusivity.

### 4.2. Conceptual model

We consider that the water concentration in Fig. 1 may be a mixture of primary and secondary water. The amount of primary water is difficult to evaluate, because the relative degrees of closed- and open-system degassing, which ultimately control the final concentration of primary water of the glass, may differ from eruption to eruption and/or from sample to sample for the same eruption (e.g., Adams et al., 2006; Wright et al., 2007; Burgisser et al., 2010; Shea et al., 2012). On the other hand, the amount of secondary water in the matrix-glass depends only on the textural characteristics of the sample and the duration between the eruption and sample analysis, provided both the solubility and the diffusivity of water are approximately constant with time, (cf. Section 4.3–4.4) and similar for all the samples. Here we investigate whether rehydration alone can account for the measured

water or not. We assume that all the samples are initially dry and progressively rehydrated with meteoric water that is always present at the vesicle/glass boundary (e.g., Friedman and Obradovich, 1981).

#### 4.3. The rehydration model

We assume a spherical geometry for vesicles and surrounding vesicle walls (e.g., see Fig. 1 of Lensky et al., 2004) and a homogeneous distribution of vesicles. Consequently, the average thickness of matrix-glass between vesicles can be estimated as  $2(S-R)$ , where  $S$  is the half-distance between the centers of two adjacent spherical vesicles of uniform size (e.g., Princen, 1979; Proussevitch et al., 1993).  $S$  depends on the vesicle radius,  $R$ , and  $\phi$  as

$$S = R/\phi^{1/3}, \quad (1)$$

where

$$R = \left( \frac{3}{4\pi N(1-\phi)} \right)^{1/3}. \quad (2)$$

Here,  $N$  is the number of vesicles per volume of solid matrix given in Table 1 for each sample.

Assuming that vesicles are interconnected (see Appendix B for a discussion on this assumption), it is to be expected that there is sufficient moisture at any time at the vesicle/glass interface for water to diffuse from the vesicle-glass interface into the matrix-glass (e.g., Ross and Smith, 1955; Friedman and Smith, 1958, 1960; Friedman et al., 1966; Friedman and Long, 1976; Friedman and Obradovich, 1981; Michels et al., 1983; Newman et al., 1986; Tuffen et al., 2010). Diffusion is assumed to take place throughout the time,  $\tau$ , between eruption and analysis (Table 1) and the rate of change in water concentration within the bubble wall can be calculated from

$$\frac{\partial c}{\partial t} = D \left( \frac{\partial^2 c}{\partial r^2} + \frac{2}{r} \frac{\partial c}{\partial r} \right). \quad (3)$$

Here  $t$  is the time,  $c(r,t)$  is water concentration in the glass,  $r$  is the radial coordinate ( $R \leq r \leq S$ ), and  $D$  is the diffusivity of water in rhyolitic glass at rehydration conditions (cf., §4.4.). The initial and boundaries conditions are

$$c = C_0 \quad \text{at} \quad R \leq r \leq S \quad \text{and} \quad t = 0, \quad (4)$$

$$\left( \frac{\partial c}{\partial r} \right)_{r=S} = 0 \quad \text{at} \quad t \geq 0, \quad (5)$$

$$c = C_R \quad \text{at} \quad r = R \quad \text{and} \quad t > 0. \quad (6)$$

We also define  $C_m(t)$  as the volumetrically averaged concentration of water in the matrix glass, where  $C_m = C_0$  at  $t=0$ , and  $C_m = C_R$  as  $t \rightarrow \infty$ .

$C_0=0.1$  wt% is the assumed concentration of water in the matrix-glass after the sample is quenched and cooled, equal to the solubility of water in the melt at atmospheric pressure and magmatic temperature of 850 °C (Liu et al., 2005). This value also corresponds to the lowest measured water concentration of any sample (Table 1, Fig. 1). The water concentration at the glass/vesicle interface,  $C_R$ , is the solubility of water in the glass at surface pressure and temperature. Hydration experiments of rhyolitic glasses at atmospheric pressure and 200 °C suggest that  $C_R \approx 2-3$  wt% (Anovitz et al., 2008), indicating that solubility increases with decreasing temperature under atmospheric pressure and sub-magmatic temperatures. Consequently, it is likely that  $C_R$  is higher than 2–3 wt% at atmospheric pressure and temperature, which is also substantiated by the high water concentrations in some of the oldest and most porous samples (i.e.,  $C_s = 3.7 \pm 0.4$  wt%), assuming that they are indeed due to rehydration. In lieu of other constraints and because of the relatively modest sensitivity

of our model predictions to  $C_R$  (Appendix B), we used a value of  $C_R=4$  wt% for all calculations.

#### 4.4. Diffusivity

Above 400 °C, water diffusion in highly silicic glasses/melts has been extensively studied and  $D$  is a well-constrained function of pressure, temperature, glass chemistry and water concentration (Zhang et al., 2007; Ni and Zhang, 2008; Ni et al., 2009a,b; Zhang and Ni, 2010; and references therein). Below 400 °C  $D$  is not as well constrained, because large diffusion times make experiments difficult. Also, at these temperatures, the inter-conversion rate between molecular  $H_2O$  and  $OH$  is greatly reduced (Michels et al., 1983) and water diffusivity is mainly controlled by the diffusivity of molecular water.

Water diffusion in obsidian is central to the discipline of *obsidian hydration dating*, where it has been studied to estimate the age of artefacts (cf. Liritzis and Laskaris, 2011, for a review). A rehydration layer forms with a thickness that scales as the square root of the product age and diffusivity because rehydration proceeds from the surface towards the interior. Apparent rehydration diffusivities in obsidians have been estimated between  $10^{-24.1}$  and  $10^{-20.9} \text{ m}^2 \text{ s}^{-1}$  (cf. Table 2), by comparing independent age estimates and measured hydration-layer thicknesses. Diffusion experiments, during which obsidian is artificially hydrated over days to months at tens of °C, have yielded apparent diffusivities of  $10^{-23.0}$ – $10^{-20.7} \text{ m}^2 \text{ s}^{-1}$ , when extrapolated to rehydration temperatures (cf. Table 2). Overall, these estimates span almost 4 orders of magnitude. By comparison, extrapolation of the diffusivity formulation for molecular water only of Ni and Zhang (2008) from  $T > 400$  °C to 25 °C and at 0.1 MPa, gives  $10^{-24.9} \text{ m}^2 \text{ s}^{-1}$  for a total water concentration of 0.1 wt% and  $10^{-18.9} \text{ m}^2 \text{ s}^{-1}$  for 4 wt% (Table 2).

Although it has been suggested that water diffusivity at very low temperatures is strongly dependent on glass chemistry, temperature, humidity and water concentration (cf. Liritzis and Laskaris, 2011), to date no self-consistent formulation exists that can explain the apparent range in water diffusivities at low temperatures. At  $T > 400$  °C the value of  $D$  is positively correlated with the total water concentration, and if the same rule applies at rehydration conditions,  $D$  should increase with time as rehydration progresses. Water diffusion coefficients measured during experimental hydration of obsidian at 90 °C by Stevenson and Novak (2011) show a decrease with time over 266 days, reinforcing the results of Anovitz et al. (2004) who showed that with progressive glass hydration  $D$  first decreases with time. However, the longer-term hydration runs by Anovitz et al. (2004) suggest that  $D$  then increases with time, as at  $T > 400$  °C. In summary, for our conditions of interest, no accepted formulation exists to relate  $D$  to water concentration, glass chemistry, temperature, humidity or any other parameter. Furthermore, the values reported in the literature span approximately 4 orders of magnitude. Therefore, our approach is to find the  $D$  that allows the best fit of our model to the data, for each eruption or for a particular eruption style. We then discuss the implications of these best  $D$  found.

#### 4.5. Non-dimensionalization

To facilitate integration of model predictions and observations (pyroclast age, porosity, vesicle number density, water concentration), we introduce the dimensionless concentration and rehydration time, respectively defined as

$$\hat{c} = \frac{c}{C_R} \quad (7)$$



**Table 2**

Diffusion coefficients of water in rhyolitic obsidians at very low temperatures and 0.1 MPa.

Approach used	Locality/total water content	Temperature (°C)	$D$ ( $\times 10^{-23} \text{ m}^2 \text{ s}^{-1}$ )	$\log D$ ( $\text{m}^2 \text{ s}^{-1}$ )	Reference
Comparison with other dating data (mainly radiocarbon)	Coastal Ecuador	30	34.9	-21.5	Friedman and Smith (1960)
	Egypt	28	25.7	-21.6	
	Southwestern USA	20–25	14–20	-21.7 to -21.8	
	Sub-Arctic	5	2.9	-22.5	Friedman and Obradovich (1981)
	Arctic	1	1.3	-22.9	
	Newberry Craters, Oregon, USA	12.6	3–10	-22.0 to -22.5	
	Salton Sea, California, USA	21.6	16	-21.8	
	Yellowstone, Wyoming, USA	4–6	6–10	-22.0 to -22.2	
	Coso Range, California, USA	25	127	-20.9	Newman et al. (1986)
	Easter Island, Chile	–	0.3–0.6	-23.2 to -23.5	Liritzis et al. (2004)
	Mykonos, Greece	–	0.3–0.6	-23.2 to -23.5	
	Hopewell, Ohio, USA	–	0.2–0.5	-23.3 to -23.7	
	Xaltocan, Mexico	–	0.1–1	-23.0 to -24.0	
	Kozushima, Japan	15–21	34–41	-21.4 to -21.5	Yokoyama et al. (2008)
	Cyclades, Greece	–	0.07–4	-22.4 to -24.1	Laskaris et al. (2011)
Greece, Asia Minor	–	0.07–1.1	-23.0 to -24.1	Liritzis et al. (2008)	
Extrapolation from experimental obsidian hydration	West Yellowstone, Montana, USA	12–16	21–63	-21.2 to -21.7	Friedman and Long (1976)
	Gardiner, Montana, USA	22.7	72	-21.1	
	Pine Mountain, Oregon, USA	11.9–24.3	1–31	-21.5 to -23.0	
	Gutierrez Zamora, Mexico	32.6	210	-20.7	
	Naivasha–Nakuru basin, Kenya	18.6	8–51	-21.3 to -22.1	Michels et al. (1983)
	Pachuca, Chalco, Basin of Mexico	19.4	33.5	-21.5	Anovitz et al. (2004)
	Hopewell, Ohio, USA	20.0	19–20	-21.7	Stevenson et al. (2004)
	Pachuca, Basin of Mexico	25	128	-20.9	Anovitz et al. (2009)
Extrapolation of the diffusivity formulation for molecular water only of Ni and Zhang (2008)	Topaz Mountain, Utah, USA	16.0	15–17	-21.8	Rogers and Duke (2011)
	Total water content=0.1 wt%	25	0.014	-24.9	Ni and Zhang (2008)
	Total water content=2.0 wt%	25	16	-21.8	
Total water content=4.0 wt%	25	13,552	-18.9		

and

$$\hat{t} = \frac{R}{S} \frac{tD}{(S-R)^2} \quad (8)$$

Here  $R$  and  $S$  are estimated from  $\phi$  and  $N$  using Eqs. (1) and (2) and  $C$  is the bulk water concentration, either modeled ( $C_m$ ) or measured ( $C_s$ ). Furthermore,  $t$  denotes the time between eruption and sample analysis. The dimensionless rehydration time,  $\hat{t}$ , reduces the dependency of rehydration from four variables, so that for a given combination of  $\phi$ ,  $N$  and  $D$ , the predicted concentration,  $\hat{C}_m$ , is a smooth function of  $\hat{t}$ , with all possible curves obtained from varying  $\phi$  and  $N$  defining the ‘rehydration trend’. Eq. (8) indicates that at high porosities ( $\phi = R^3/S^3 \sim 1$ ), time is approximately scaled by the characteristic diffusion time of a plane sheet of thickness  $S - R$ , whereas at small porosities ( $R \ll S$ ), time is approximately scaled by  $R/S^3$ .

Fig. 2 illustrates the utility of non-dimensionalizing time. Using Eqs. (1)–(3), we calculated the rehydration of 10 hypothetical samples comprising different combinations of porosity, bubble number density and rehydration time. The individual rehydration curves of Fig. 2a reduce to a single ‘rehydration trend’, when plotted in dimensionless time and concentration (Fig. 2b). Consequently, water concentrations of initially dry samples of different ages, porosities and vesicle number densities should, after rehydration, plot along a single rehydration trend (assuming a constant diffusivity). Samples with a large fraction of primary water, or that have not undergone rehydration, should for the most part plot above or below this rehydration trend, respectively.

## 5. Model results and discussion

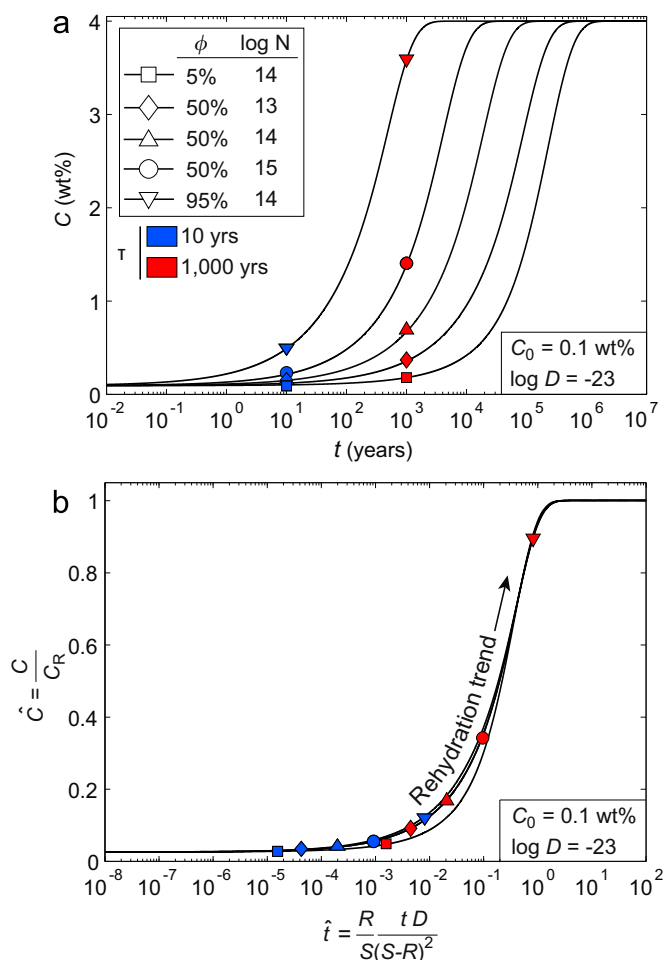
### 5.1. Rehydration trend and measured water concentrations

Fig. 3 shows water concentrations from individual eruptions (Fig. 3a–d) and eruptive styles (Fig. 3e–f) relative to the rehydration trend for a value of  $D$  that minimizes (non-weighted least squares) the root-mean-square deviation (RMSD) between measured and predicted water concentrations. For each case, an initially degassed sample was assumed to rehydrate, starting at a water concentration of  $C_0 = 0.1$  wt% and at a value of  $C_R = 4$  wt%.

Most of the data can be explained by the rehydration of a degassed sample at an average rehydration diffusivity of approximately  $10^{-23.0 \pm 1.2} \text{ m}^2 \text{ s}^{-1}$ , except samples from the pre-climatic phase of Pinatubo 1991 eruption (see dark gray squares in Fig. 3a–f). The best-fit diffusivities range from  $10^{-22.0 \pm 0.2} \text{ m}^2 \text{ s}^{-1}$  for the 1997 eruptions of Soufrière Hills to  $10^{-23.8 \pm 0.4} \text{ m}^2 \text{ s}^{-1}$  for the 1100 AD eruption of Medicine Lake and the 79 AD eruption of Vesuvius eruption. The sensitivity of our results on diffusivity,  $D$ , assumed initial water concentration,  $C_0$ , and assumed solubility,  $C_R$ , are shown in Appendix B and Fig. B1a.

### 5.2. Primary water and open-system degassing

The estimated average rehydration diffusivity of  $10^{-23} \text{ m}^2 \text{ s}^{-1}$  falls within the range of estimates from obsidian hydration dating ( $10^{-24.1} - 10^{-20.7} \text{ m}^2 \text{ s}^{-1}$ ), as well as the range obtained from extrapolation of molecular water diffusivity to 25 °C and atmospheric pressure ( $10^{-24.9} - 10^{-18.9} \text{ m}^2 \text{ s}^{-1}$ ; Ni and Zhang, 2008; cf. Table 2). Although some variability in diffusivity due to chemistry, surface



**Fig. 2.** Predicted water concentrations due to rehydration as a function of time in dimensional (a) or dimensionless (b) values for five hypothetical samples. Values of porosity and bubble number density are  $\phi=5\%$ , 50%, 95%, and  $N=10^{13}$ ,  $10^{14}$ ,  $10^{15} \text{ m}^{-3}$ . The samples have an initial concentration of  $C_0=0.1$  wt% and  $D$  is assumed to be constant and equal to  $10^{-23} \text{ m}^2 \text{ s}^{-1}$ . Water concentrations predicted after 10 and 1000 yr are shown on both graphs. In dimensionless coordinates, the water concentrations collapse to a well-defined rehydration trend. Any sample plotting above this rehydration trend would require either that  $C_0 > 0.1$  wt% and/or that  $D > 10^{-23} \text{ m}^2 \text{ s}^{-1}$ .

temperature, water concentration and humidity is to be expected (cf. Liritzis and Laskaris, 2011 and references therein), our results suggest that this variability is relatively small, at least over time periods of years and greater.

Although some fraction of primary water is likely present in most samples, the correlation between sample porosity and water concentrations (Fig. 1) can mostly be attributed to rehydration (Fig. 3). Consequently, we suggest that most samples must have lost a large percentage of their primary water upon eruption. In many cases this probably requires extensive open-system degassing at some stage during eruption.

For example, all samples from effusive, dome-forming eruptions have low porosities and water concentrations that are lower than theoretical predictions from closed-system equilibrium degassing models (Fig. 4). The low porosity of such samples, known to have originated from water-rich magmas, is attributed to open-system degassing and bubble collapse during slow ascent to the surface and emplacement within the dome (e.g., Eichelberger et al., 1986; Newman et al., 1988; Westrich et al., 1988; Westrich and Eichelberger, 1994; Stasiuk et al. 1996; Villemant and Boudon, 1999; Gonnermann and Manga, 2003,

2005, 2007; Melnik and Sparks, 2005; Mueller et al., 2005; Okumura et al., 2009; Takeuchi et al., 2009; Wright et al., 2009; Castro et al., 2012). However, because of the low surface area to volume ratio of these samples, rehydration is slow (Eq. (8)), the concentration of secondary water in the samples considered in our study is limited to values of approximately 1.5 wt% or less.

In contrast, water concentrations in samples from Vulcanian and (sub)Plinian eruptions tend to be higher than for effusive eruptions (Fig. 4), with (sub)Plinian samples distinctly having the highest porosities and water concentrations. Although our analysis cannot determine the precise proportion of primary and secondary water, Fig. B1c (Appendix B) shows that the model permits primary water contents of approximately 10–30%, assuming that the amount of primary water does not vary randomly, but is proportional to the total water concentration of the sample. The analyzed explosive samples tend to span the full range in water concentrations and they fall along a rehydration trend. For example, pumices from the climax of the 1991 AD Pinatubo eruption (Gerlach et al., 1996; Fig. 1), collected only 6 months after the eruption, contain approximately 0.3 wt% water. Therefore, the simplest interpretation is that the Vulcanian and (sub) Plinian sample also underwent considerable open-system degassing upon eruption, with present-day water concentrations largely a consequence of rehydration. However, the question of how much open-system degassing takes place prior to or upon magma fragmentation during these explosive eruptions remains a topic of debate. Our results suggest that if a large fraction of water remains dissolved in the melt at the time of magma fragmentation (e.g., Gonnermann and Houghton, 2012), much of it may be lost as a consequence of open-system degassing within the time interval between fragmentation and quenching (e.g., Thomas et al., 1994; Gardner et al., 1996; Rust and Cashman, 2004, 2011; Gonnermann and Houghton, 2012).

In contrast, the samples of the pre-climatic Vulcanian phase of Pinatubo in 1991 cannot be matched to a rehydration trend with  $D \sim 10^{-23} \text{ m}^2 \text{ s}^{-1}$ . The most reasonable interpretation seems the retention of more than 1 wt% of primary water, interpreted as being inherited from the densification of highly vesicular pumices, due to open-system degassing and bubble collapse during the repose period between two successive eruptions (Hammer et al., 1999). It should be noted that although the samples from the 1997 eruptions of Soufrière Hills closely match a rehydration trend, the high water concentrations of some of these samples have been interpreted similarly as primary due to incomplete magma degassing (Burgisser et al., 2010; Giachetti et al., 2010).

### 5.3. Permeability threshold

A feature that stands out in Fig. 4 is the absence of data at water concentrations above 1.5–2 wt% and porosities below approximately 30–40%. We interpret this within the context of a permeability threshold (e.g., Eichelberger et al., 1986; Candela, 1991; Sahimi, 1994; Garboczi et al., 1995; Saar and Manga, 1999; Gaonach et al., 2003; Mueller et al., 2005; Takeuchi et al., 2005, 2008, 2009; Namiki and Manga, 2008; Polacci et al., 2008; Walsh and Saar, 2008; Rust and Cashman, 2011), with a porosity of 30–40% representing a minimum bound for this threshold. Consequently, open-system degassing will not commence until a sample has reached a porosity of at least 30–40% or higher (Eichelberger et al., 1986; Takeuchi et al., 2005, 2008, 2009; Namiki and Manga, 2008; Rust and Cashman, 2011).

At values below this threshold permeability is either negligible, or sufficiently small, so that the characteristic time scale for open-system degassing is much greater than either the characteristic

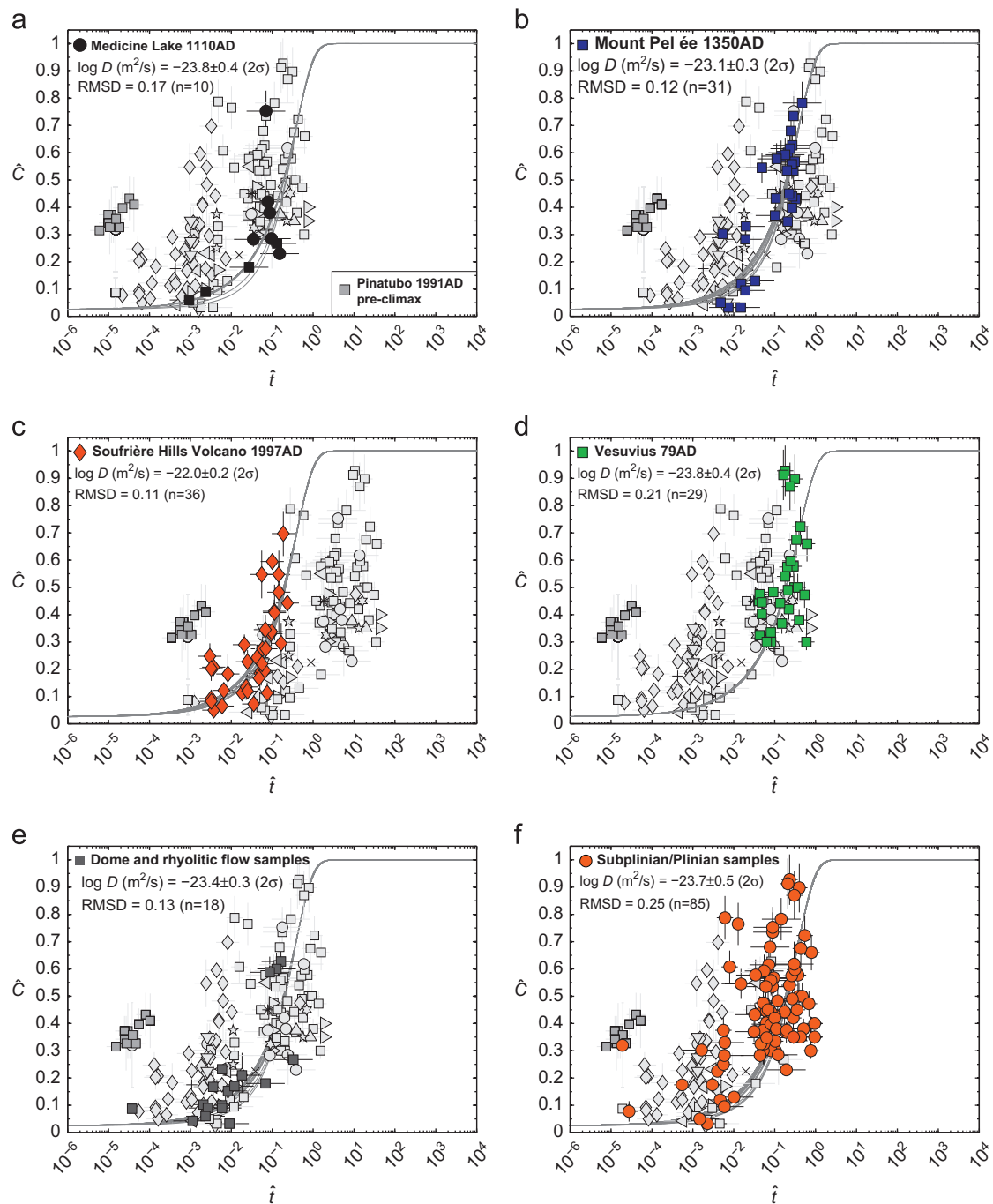


**Fig. 3.** Best least-squares fit of dimensionless water concentration to a rehydration trend defined by one value of  $D$  and values of  $C_0=0.1$  wt%, as well as  $C_R=4$  wt%. Each plot is for a given eruption (a–d) or for a particular eruption style (e–f), as labeled. For each case the best fit was obtained by varying  $D$  to minimize  $\sqrt{\sum_{i=1}^n (\hat{C}_s - \hat{C}_m)^2 / n}$ , with  $n$  the number of samples,  $\hat{C}_s$  defined in Eq. (7), and  $\hat{C}_m$  the modeled dimensionless concentration interpolated for  $t=\tau$ . The data fitted are shown in color and the other data are in gray. Note that the samples from the Vulcanian pre-climax phase of the Pinatubo's 1991 eruption (highlighted in dark gray; Hammer et al., 1999) are outliers on the six graphs. Fitting them while keeping  $C_0=0.1$  wt% would require  $D=10^{-19.9}$  m<sup>2</sup> s<sup>-1</sup>, which is 3 orders of magnitude higher than the average  $D=10^{-23}$  m<sup>2</sup> s<sup>-1</sup> required to fit all other samples. (For interpretation of the references to color in this figure legend, the reader is referred to the web version of this article.)

decompression time (e.g., Lensky et al., 2004), or the sample's quench time after fragmentation (e.g., Gonnermann and Houghton, 2012). The implication of such a threshold is that samples with porosities of less than 30% will have been subjected to bubble collapse during open-system degassing (Klug et al., 2002; Rust and Cashman, 2004; Mueller et al., 2005; Gurioli et al., 2005; Wright and Weinberg, 2009; Houghton et al., 2010), and would therefore have been previously more vesicular.

## 6. Conclusion

We compiled and collected 163 matrix-glass water concentration measurements of samples with intermediate to highly silicic compositions and eruption styles that range in intensity from dome to Plinian eruptions. The concentration in water ranges from 0.1 wt% to more than 3.5 wt% and is positively correlated with porosity. From rehydration modeling, we find that most of the

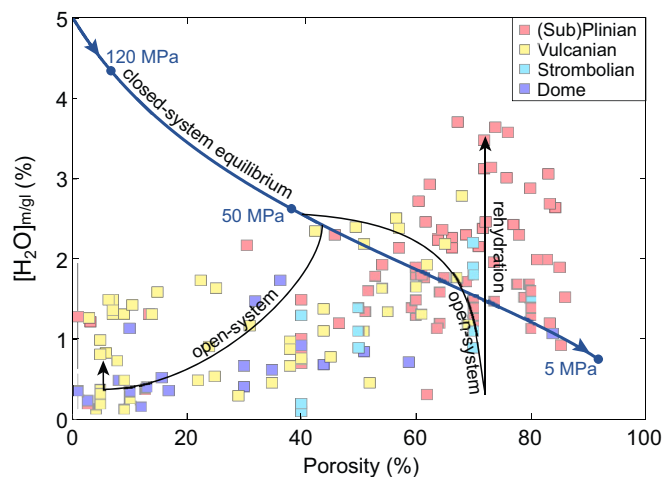


**Fig. 4.** Diagram illustrating the relationship between sample porosity and water concentration, a hypothetical closed-system equilibrium degassing trend, as well as several hypothetical open-system degassing together with subsequent rehydration trends. The data are grouped by eruption style. The equilibrium closed-system degassing trend is for an initial water concentration of 5 wt%, assuming a melt density of  $2500 \text{ kg m}^{-3}$ , ideal gas law and water solubility of Liu et al. (2005). Gas pressures are indicated along this curve. A necessary requirement for a path above the equilibrium closed-system trend is kinetic disequilibrium. A necessary requirement for a degassing path below the equilibrium curve is open-system degassing. Note that the possibility of bubble resorption (Westrich and Eichelberger, 1994; Yoshimura and Nakamura, 2008, 2010; Watkins et al., 2012; McIntosh et al., 2013) is not accounted for in this figure.

water measured in these samples can be explained by rehydration, the post-eruptive diffusion of external water at atmospheric temperature and pressure, except those from the Vulcanian pre-climactic eruption of Pinatubo in 1991. We find that rehydration over a wide range in time scales ( $\sim 1$  to  $> 10^4$  yr) can be characterized by an average diffusivity of approximately  $10^{-23} \text{ m}^2 \text{ s}^{-1}$ .

Although the precise proportion of primary (magmatic) to secondary (meteoric) water cannot be determined by our analysis, our model suggests that most of the samples were extensively degassed during eruption, confirming the importance of open-system degassing. We interpret the absence of samples with high water concentration and porosities of less than 30–40% as a lower bound on the permeability threshold for open-system degassing.

## Acknowledgments

This study benefitted from discussions with L.M. Anovitz, J.E. Gardner, M. Humphreys, N. Laskaris, A. Lutge, T. Shea and H. Tuffen. We thank B.F. Houghton for providing Novarupta samples and Netzsch Instruments North America for TGA-MS analyses. We also thank H. Wright and one anonymous reviewer for comments and suggestions that helped improving this manuscript. TG and HMG were supported by NSF grants EAR-1019872 and IDR-1015069.

## Appendix A. Methods used to measure $\phi$ and $C_s$ in this study

The 10 pumices and obsidians from the 1110 AD eruption of Medicine Lake Volcano (MLV) were collected in October 2011. Sample porosity was determined by helium pycnometry following the same procedure as in Giachetti et al. (2010). Matrix-glass water concentrations were measured by TGA, on a TA Instruments Q600, at Rice University, Houston. Each pyroclast was crushed and

sieved, and only the grains with sizes smaller than  $37 \mu\text{m}$  were analyzed. MLV pyroclasts did not undergo any pre-analysis heating. Therefore, if present, any secondary water was not removed from the samples prior to analysis. Approximately 20 mg of the pyroclast powder was placed in a tarred alumina cup on the TGA sample beam and heated at  $10 \text{ }^\circ\text{C min}^{-1}$  from ambient temperature to  $1250 \text{ }^\circ\text{C}$ , and then held at this temperature for 1 h. During analysis, the sample was purged by nitrogen with better than 99.997% purity, at a flux of  $150 \text{ ml min}^{-1}$ . Total water mass was obtained by subtracting the final weight of the sample powder to its initial weight, assuming that water is the ultra-dominant volatile species exsolved. One pumice clast and one obsidian piece, each, were analyzed with a TGA coupled to a mass spectrometer, by Netzsch Company, the evolved gases being analyzed at each time step with a Netzsch QMS 403 Aeolos system coupled to the TGA. Results show that water represents more than 95% of the volatiles exsolved during analysis.

The three pumices from the 1912 Plinian eruption of Novarupta were collected in 2003 by Houghton and Adams (Adams et al., 2006), with porosities reported in Adams et al. (2006) following the method of Houghton and Wilson (1989). Evans Analytical Group measured the matrix-glass H concentration of these clasts using Instrumental Gas Analysis. Samples were crushed and tens of mg were placed in a graphite crucible and inserted into an electrode furnace. The crucible is maintained between the upper and lower electrodes of impulse furnace. A high current passes through the crucible after purging with inert gas creating a  $\approx 2000 \text{ }^\circ\text{C}$  zone in which carbothermal reduction occurs. Gases generated are released into flowing inert gas stream, which is then sent to a thermal conductivity TCD detector to quantify H.  $C_s$  is then calculated using H mass fraction, assuming H is in the form  $\text{H}_2\text{O}$  only.

## Appendix B. Sensitivity of the model on the values of $D$ , $C_R$ , $C_0$ and vesicle connectivity

We investigated the sensitivity of our model predictions to  $D$  and  $C_R$  by varying  $C_R$  from 4 to 10 wt% (highest water concentration given by Denton et al. (2009) in obsidians and perlitites) at a constant value of  $D = 10^{-23} \text{ m}^2 \text{ s}^{-1}$  and by varying  $D$  between  $10^{-25}$  and  $10^{-19} \text{ m}^2 \text{ s}^{-1}$ , at a constant value of  $C_R = 4 \text{ wt}\%$ . The sensitivity of our model predictions to  $D$  is illustrated in Fig. B1a, which indicates that at any given value of  $C_R$ , the root-mean-square deviation (RMSD) between measured and predicted water concentrations defines a well-constrained minimum. Although, there is a tradeoff between  $D$  and  $C_R$  (Fig. B1b), the uncertainty in the estimate of  $D$  is relatively modest and unlikely to significantly change our conclusions.

We also investigated the sensitivity of our model to the value of the primary water concentration of each sample,  $C_0$ . We assumed that, for all the samples of a particular eruption,  $C_0$  is a constant fraction of the measured water concentration (i.e.,  $\alpha = C_0/C = \text{constant}$ ). For each eruption in Fig. B1a, we used the best  $D$  found, we varied  $\alpha$  from 0 to 1 and calculated the RMSD. The RMSD is minimum for primary water concentration that represents from 10% (Soufrière Hills 1997 AD) to 32% (Vesuvius 79 AD) of the total water concentration measured in the samples.

In our model, we assume that characteristic thickness of the rehydrating glass that surrounds individual vesicles depends on the reported bulk porosity,  $\phi$ , and on bubble number density,  $N$ . Because water is only in contact with the glass, if the vesicle is connected to the exterior, the use of bulk porosity instead of connected porosity may result in a slight overestimate in rehydration. For those samples where both connected and bulk porosity were measured, we find that connected porosity is on average only

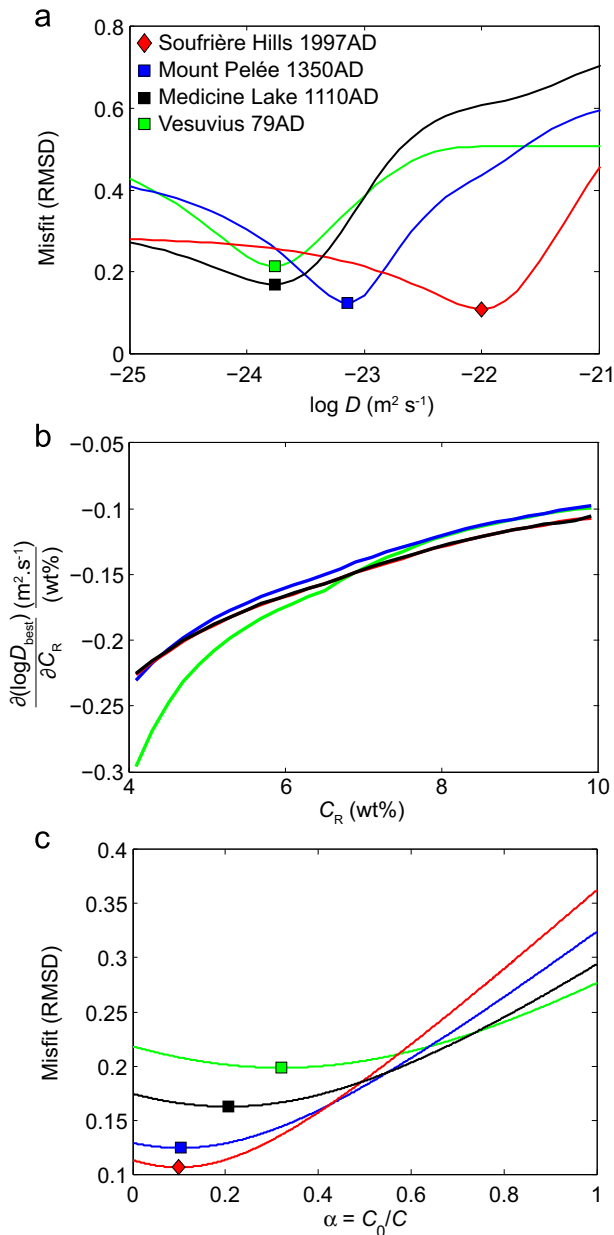


**Fig. B1.** (a) Root-mean-square deviation (RMSD) between measured and predicted water concentrations as a function of  $D$  at constant  $C_0=0.1$  wt% and  $C_R=4$  wt% for four of the eruptions studied. (b) Variation of  $\partial D/\partial C_R$  as a function of  $C_R$  at constant  $D=10^{-23} \text{ m}^2 \text{ s}^{-1}$  and  $C_0=0.1$  wt%. (c) RMSD between measured and predicted water concentrations as a function of  $\alpha=C_0/C$  at constant  $C_R=4$  wt%, and using the best  $D$  for each eruption.

5–12% lower than bulk porosity. The resultant difference in predicted water content scales accordingly and affects our results only negligibly.

## References

- Adams, N.K., Houghton, B.F., Hildreth, W., 2006. Abrupt transitions during sustained explosive eruptions: examples from the 1912 eruption of Novarupta, Alaska. *Bull. Volcanol.* 69, 189–206.
- Anderson, A.T., 1974. Chlorine, sulfur, and water in magmas and oceans. *GSA Bull.* 85 (9), 1485–1492.
- Anovitz, L.M., Elam, J.M., Riciputi, L.R., Cole, D.R., 1999. The failure of obsidian-hydration-dating: sources, implications, and new directions. *J. Archaeol. Sci.* 26 (7), 735–752.
- Anovitz, L.M., Elam, J.M., Riciputi, L.R., Cole, D.R., 2004. Isothermal time-series determination of the rate of  $\text{H}_2\text{O}$  diffusion in Pachuca Obsidian. *Archaeometry* 46, 301–326.
- Anovitz, L.M., Riciputi, L.R., Cole, D.R., Elam, J.M., Gruskiewicz, M.S., 2006. The effect of changes in relative humidity on the hydration rate of Pachuca obsidian. *J. Non-Cryst. Solids* 352, 5652–5662.
- Anovitz, L.M., Cole, D.R., Fayek, M., 2008. Mechanisms of rhyolitic glass hydration below the glass transition. *Am. Mineral.* 93 (7), 1166–1178.
- Anovitz, L.M., Cole, D.R., Riciputi, L.R., 2009. Low-temperature isotopic exchange in obsidian: implications for diffusive mechanisms. *Geochim. Cosmochim. Acta* 73, 3795–3806.
- Bacon, C.R., Newman, S., Stolper, E., 1992. Water,  $\text{CO}_2$ , Cl, and F in melt inclusions in phenocrysts from three Holocene explosive eruptions, Crater Lake, Oregon. *Am. Mineral.* 77, 1021–1030.
- Balcone-Boissard, H., Villemant, B., Boudon, G., Michel, A., 2008. Non-volatile vs. volatile behaviours of halogens during the AD 79 plinian eruption of Mt. Vesuvius, Italy. *Earth Planet. Sci. Lett.* 269, 66–79.
- Balcone-Boissard, H., Boudon, G., Villemant, B., 2011. Textural and geochemical constraints on eruptive style of the 79 AD eruption at Vesuvius. *Bull. Volcanol.* 73, 279–294.
- Barberi, F., Bizouard, H., Clochiatti, R., Metrich, N., Santacroce, R., Sbrana, A., 1981. The Somma-Vesuvius magma chamber: a petrological and volcanological approach. *Bull. Volcanol.* 44, 3.
- Barclay, J., Rutherford, M.J., Carroll, M.R., Murphy, M.D., Devine, J.D., Gardner, J.E., Sparks, R.S.J., 1998. Experimental phase equilibria constraints on pre-eruptive storage conditions of the Soufrière Hills magma. *Geophys. Res. Lett.* 25, 3437–3440.
- Bernard, A., Knittel, U., Weber, B., Weis, D., Albrecht, A., Hattori, K., Klein, J., Oles, D., 1996. Petrology and geochemistry of the 1991 eruption products of Mount Pinatubo. In: Newhall, C.G., Punongbayan, R.S. (Eds.), *Fire and Mud: Eruptions and Lahars of Mount Pinatubo*, Philippines. University of Washington Press, Seattle, pp. 767–797.
- Bertagnini, A., Landi, P., Rosi, M., Vigliarigo, A., 1998. The Pomice di Base plinian eruption of Somma-Vesuvius. *J. Volcanol. Geotherm. Res.* 83, 219–239.
- Blank, J.G., Stolper, E.M., Carroll, M.R., 1993. Solubilities of carbon dioxide and water in rhyolitic melt at 850 °C and 750 bars. *Earth Planet. Sci. Lett.* 119, 27–36.
- Blundy, J., Cashman, K.V., 2005. Rapid decompression driven crystallization recorded by melt inclusions from Mount St. Helens volcano. *Geology* 33 (10), 793–796.
- Blundy, J., Cashman, K.V., Humphreys, M., 2006. Magma heating by decompression-driven crystallization beneath andesite volcanoes. *Nature* 443, 76–80.
- Burgisser, A., Gardner, J.E., 2005. Experimental constraints on degassing and permeability in volcanic conduit flow. *Bull. Volcanol.* 67, 42–56.
- Burgisser, A., Poussineau, S., Arbaret, L., Druitt, T.H., Giachetti, T., Bourdier, J.-L., 2010. Pre-explosive conduit conditions of the 1997 Vulcanian explosions at Soufrière Hills Volcano (Montserrat): I. Pressure and vesicularity distributions. *J. Volcanol. Geotherm. Res.* 194 (1–3), 27–41.
- Burnham, C.W., 1975. Water and magmas: a mixing model. *Geochim. Cosmochim. Acta* 39, 1077–1084.
- Candela, P.A., 1991. Physics of aqueous phase evolution in plutonic environments. *Am. Mineral.* 76, 1081–1091.
- Castro, J.M., Cordonnier, B., Tuffen, H., Tobin, M.J., Puskar, L., Martin, M.C., Bechtel, H.A., 2012. The role of melt-fracture degassing in defusing explosive rhyolite eruptions at volcan Chaiten. *Earth Planet. Sci. Lett.* 333–334, 63–69.
- Civetta, L., Orsi, G., Pappalardo, L., Fisher, R.V., Heiken, G., Ort, M., 1997. Geochemical zoning, mingling, eruptive dynamics and depositional processes – the Campanian Ignimbrite, Campi Flegrei caldera, Italy. *J. Volcanol. Geotherm. Res.* 75, 183–219.
- Clarke, A.B., Stephens, S., Teasdale, R., Sparks, R.S.J., Diller, K., 2007. Petrologic constraints on the decompression history of magma prior to Vulcanian eruptions at the Soufrière Hills volcano, Montserrat. *J. Volcanol. Geotherm. Res.* 161, 261–274.
- DeGroot-Nelson, P.J., Cameron, B.I., Fink, J.H., Holloway, J.R., 2001. Hydrogen isotope analysis of rehydrated silicic lavas: implications for eruption mechanisms. *Earth Planet. Sci. Lett.* 185, 331–341.
- Denton, J.S., Tuffen, H.J., Gilbert, S., Odling, N., 2009. The hydration and alteration of perlite and rhyolite. *J. Geol. Soc. London* 166, 895–904.
- Denton, J.S., Tuffen, H.J., Gilbert, S., 2012. Variations in hydration within perlitised rhyolitic lavas—evidence from Torfajökull, Iceland. *J. Volcanol. Geotherm. Res.* 223–224, 64–73.
- Di Muro, A., Villemant, B., Montagnac, G., Scaillet, B., Reynard, B., 2006. Quantification of water content and speciation in natural silicic glasses (phonolite, dacite, rhyolite) by confocal microRaman spectrometry. *Geochim. Cosmochim. Acta* 70, 2868–2884.
- D’Orlando, C., Poggianti, E., Bertagnini, A., Cioni, R., Landi, P., Polacci, M., Rosi, M., 2005. Changes in eruptive style during the A.D. 1538 Monte Nuovo eruption (Phlegrean Fields, Italy): the role of syn-eruptive crystallization. *Bull. Volcanol.* 67 (7), 601–621.
- Donnelly-Nolan, J.M., Grove, T.L., Lanphere, M.A., Champion, D.E., Ramsey, D.W., 2008. Eruptive history and tectonic setting of Medicine Lake Volcano, a large rear-arc volcano in the southern Cascades. *J. Volcanol. Geotherm. Res.* 177, 313–328.
- Eichelberger, J.C., Carrigan, C.R., Westrich, H.R., Price, R.H., 1986. Non-explosive silicic volcanism. *Nature* 323, 598–602.
- Friedman, L., Smith, R.L., 1958. The deuterium content of water in some volcanic glasses. *Geochim. Cosmochim. Acta* 15, 218–228.
- Friedman, I., Smith, R.L., 1960. A new dating method using obsidian: Part 1, the development of the method. *Am. Antiquity* 25, 476–522.
- Friedman, I., Smith, R.L., Long, W.D., 1966. Hydration of natural glass and formation of perlite. *Geol. Soc. Am. Bull.* 77, 323–328.

- Friedman, I., Long, W., 1976. Hydration rate of obsidian. *Science* 191, 347–352.
- Friedman, I., Obradovich, J., 1981. Obsidian hydration dating of volcanic events. *Quat. Res.* 16, 37–47.
- Fuglignati, P., Marianelli, P., Proto, M., Sbrana, A., 2004. Evidences for disruption of a crystallizing front in a magma chamber during caldera collapse: an example from the Breccia Museo unit (Campanian Ignimbrite eruption, Italy). *J. Volcanol. Geotherm. Res.* 133, 141–155.
- Gaonach, H., Lovejoy, S., Schertzer, D., 2003. Percolating magmas and explosive volcanism. *Geophys. Res. Lett.* 30 (11), 1559.
- Garboczi, E.J., Snyder, K.A., Douglas, J.F., Thorpe, M.F., 1995. Geometrical percolation threshold of overlapping ellipsoids. *Phys. Rev. E* 52, 819–828.
- Gardner, J.E., Thomas, R.M.E., Jaupart, C., Tait, S., 1996. Fragmentation of magma during Plinian volcanic eruptions. *Bull. Volcanol.* 58, 144–162.
- Gerlach, T.M., Westrich, H.R., Symonds, R.B., 1996. Pre-eruption vapor in magma of the climatic Mount Pinatubo eruption: source of the giant stratospheric sulfur dioxide cloud. In: Newhall, C.G., Punongbayan, R.S. (Eds.), *Fire and Mud: Eruptions and Lahars of Mount Pinatubo, Philippines*. University of Washington Press, Seattle, pp. 415–433.
- Giachetti, T., Druitt, T.H., Burgisser, A., Arbaret, L., Galven, C., 2010. Bubble nucleation and growth during the 1997 Vulcanian explosions of Soufrière Hills Volcano, Montserrat. *J. Volcanol. Geotherm. Res.* 193 (3–4), 215–231.
- Gonnermann, H.M., Manga, M., 2003. Explosive volcanism may not be an inevitable consequence of magma fragmentation. *Nature* 426, 432–435.
- Gonnermann, H.M., Manga, M., 2005. Nonequilibrium magma degassing: results from modeling of the ca. 1340 AD eruption of Mono Craters, California. *Earth Planet. Sci. Lett.* 238, 1–16.
- Gonnermann, H.M., Manga, M., 2007. The fluid mechanics of volcanic eruptions. *Annu. Rev. Fluid Mech.* 39, 321–356.
- Gonnermann, H.M., Houghton, B.F., 2012. Magma degassing during the Plinian eruption of Novarupta, Alaska, 1912. *Geochem. Geophys. Geosyst.* 13, Q10009.
- Gurioli, L., Houghton, B.F., Cashman, K.V., Cioni, R., 2005. Complex changes in eruption dynamics during the 79 AD eruption of Vesuvius. *Bull. Volcanol.* 67, 144–159.
- Hammer, J.E., Cashman, K.V., Hoblitt, R.P., Newman, S., 1999. Degassing and microlite crystallization during pre-climatic events of the 1991 eruption of Mt. Pinatubo, Philippines. *Bull. Volcanol.* 60, 355–380.
- Hammer, J.E., Rutherford, M.J., 2002. An experimental study of the kinetics of decompression-induced crystallization in silicic melt. *J. Geophys. Res.* 107, 1–24.
- Harford, C.L., Sparks, R.S.J., Fallick, A.E., 2003. Degassing at the Soufrière Hills Volcano, Montserrat, recorded in matrix glass compositions. *J. Petrol.* 44, 1503–1523.
- Heiken, G., 1978. Plinian-type eruptions in the Medicine Lake Highland, California, and the nature of the underlying magma. *J. Volcanol. Geotherm. Res.* 4, 375–402.
- Heiken, G., Wohletz, K., 1987. Tephra deposits associated with silicic domes and lava flows. *Geol. Soc. Am., Spec. Pap.* 212, 55–76.
- Hildreth, W., 1983. The compositionally zoned eruption of 1912 in the Valley of Ten Thousand Smokes, Katmai National Park, Alaska. *J. Volcanol. Geotherm. Res.* 18, 1–56.
- Hildreth, W., Fierstein, J., 2012. The Novarupta–Katmai Eruption of 1912—Largest Eruption of the Twentieth Century; Centennial Perspectives. *US Geological Survey Professional vol.* 1791, 259 pp.
- Holloway, J.R., Blank, J.G., 1994. Application of experimental results to C–O–H series in natural melts. *Rev. Mineral.* 30, 187–230.
- Houghton, B.F., Wilson, C.J.N., 1989. A vesicularity index for pyroclastic deposits. *Bull. Volcanol.* 51, 451–462.
- Houghton, B.F., Carey, R.J., Cashman, K.V., Wilson, C.J.N., Hobden, B.J., Hammer, J.E., 2010. Diverse patterns of ascent, degassing, and eruption of rhyolite magma during the 1.8 ka Taupo eruption, New Zealand: evidence from clast vesicularity. *J. Volcanol. Geotherm. Res.* 195 (1), 31–47.
- Ihinger, P.D., Hervig, R.L., McMillan, P.F., 1994. Analytical methods for volatiles in glasses. *Rev. Mineral. Geochem.* 30, 67–121.
- Isia, R., D'Antonio, M., Dell'Erba, F., Di Vito, M., Orsi, G., 2004. The Astroni volcano: the only example of closely spaced eruptions in the same vent area during the recent history of the Campi Flegrei caldera (Italy). *J. Volcanol. Geotherm. Res.* 131, 171–192.
- Jaupart, C., Allègre, C.J., 1991. Gas content, eruption rate and instabilities of eruption regime in silicic volcanoes. *Earth Planet. Sci. Lett.* 102, 413–429.
- Johnson, M.C., Anderson, A.T., Rutherford, M.J., 1994. Pre-eruptive volatile contents of magmas. In: Carroll, M.R., Holloway, J.R. (Eds.), *Volatiles in Magmas*. *Reviews in Mineralogy vol.* 30, pp. 281–330.
- Klug, C., Cashman, K.V., 1994. Vesiculation of May 18, 1980, Mount St. Helens magma. *Geology* 22, 468–472.
- Klug, C., Cashman, K.V., 1996. Permeability development in vesiculating magmas: implications for fragmentation. *Bull. Volcanol.* 58, 87–100.
- Klug, C., Cashman, K.V., Bacon, C.R., 2002. Structure and physical characteristics of pumice from the climatic eruption of Mount Mazama (Crater Lake), Oregon. *Bull. Volcanol.* 64, 486–501.
- Laskaris, N., Sampson, A., Mavridis, F., Liritzis, I., 2011. Late Pleistocene/Early Holocene seafaring in the Aegean: new obsidian hydration dates with the SIMS-SS method. *J. Archaeol. Sci.* 38, 2475–2479.
- Lensky, N.G., Navon, O., Lyakhovskiy, V., 2004. Bubble growth during decompression of magma: experimental and theoretical investigation. *J. Volcanol. Geotherm. Res.* 129, 7–22.
- Liritzis, I., Diakostamatiou, M., Stevenson, C.M., Novak, S.W., Abdelrehim, I., 2004. Dating of hydrated obsidian surfaces by SIMS-SS. *J. Radioanal. Nucl. Chem.* 261 (i), 51–60.
- Liritzis, I., Bonini, M., Laskaris, N., 2008. Obsidian hydration dating by SIMS-SS: surface suitability criteria from atomic force microscopy. *Surf. Interface Anal.* 40, 458–463.
- Liritzis, I., Laskaris, N., 2011. Fifty years of obsidian hydration dating in archaeology. *J. Non-Cryst. Solids* 357, 2011–2023.
- Liu, Y., Zhang, Y., Behrens, H., 2005. Solubility of H<sub>2</sub>O in rhyolitic melts at low pressures and a new empirical model for mixed H<sub>2</sub>O–CO<sub>2</sub> solubility in rhyolitic melts. *J. Volcanol. Geotherm. Res.* 143, 219–235.
- Lowenstern, J.B., 1995. Applications of silicate melt inclusions to the study of magmatic volatiles. In: Thompson, J.F.H. (Ed.) *Magmas, Fluids and Ore Deposits*. Mineralogical Association of Canada Short Course. vol. 23, pp. 71–99.
- Lowenstern, J.B., 2003. Melt inclusions come of age: volatiles, volcanoes, and Sorby's legacy. *Dev. Volcanol.* 5, 1–21.
- Mangan, M.T., Sisson, T.W., 2000. Delayed, disequilibrium degassing in rhyolite magma: decompression experiments and implications for explosive volcanism. *Earth Planet. Sci. Lett.* 183, 441–455.
- Martel, C., Bourdier, J.-L., Pichavant, M., Traineau, H., 2000. Textures, water content and degassing of silicic andesites from recent plinian and dome-forming eruptions at Mount Pelée volcano (Martinique, Lesser Antilles arc). *J. Volcanol. Geotherm. Res.* 96, 191–206.
- Martel, C., Poussineau, S., 2007. Diversity of eruptive styles inferred from the microlites of Mt Pelée andesite (Martinique, Lesser Antilles). *J. Volcanol. Geotherm. Res.* 166, 233–254.
- Massol, H., Koyaguchi, T., 2005. The effect of magma flow on nucleation of gas bubbles in a volcanic conduit. *J. Volcanol. Geotherm. Res.* 143, 69–88.
- Mastrolorenzo, G., Pappalardo, L., 2006. Magma degassing and crystallization processes during eruptions of high-risk Neapolitan-volcanoes: evidence of common equilibrium rising processes in alkaline magmas. *Earth Planet. Sci. Lett.* 250, 164–181.
- McIntosh, I., Lewellin, E., Humphreys, M., Burgisser, A., Schipper, I., Nichols, A., 2013. Dissolved H<sub>2</sub>O distribution in vesicular magmatic glass records quench history and challenges emerging paradigm. *Geophysical Research Abstracts*. EGU2013-3305.
- Melnik, O., Sparks, R.S.J., 2005. Dynamics of magma flow inside volcanic conduits with bubble overpressure buildup and gas loss through permeable magma. *J. Volcanol. Geotherm. Res.* 143, 53–68.
- Michels, J.W., Tsong, I.S.T., Nelson, C.M., 1983. Obsidian dating and East African archeology. *Science* 219, 361–366.
- Moitra, P., Gonnermann, H.M., Houghton, B.F., Giachetti, T., 2013. Relating vesicle shapes in pyroclasts to eruption styles. *Bull. Volcanol.* 75, 691.
- Moore, G., Vennemann, T., Carmichael, I.S.E., 1995. The solubility of water in natural silicate melts to 2 kilobars. *Geology* 23, 1009–1102.
- Moore, G., Vennemann, T., Carmichael, I.S.E., 1998. An empirical model for the solubility of H<sub>2</sub>O in magmas to 3 kilobars. *Am. Mineral.* 83, 36–42.
- Mueller, S., Melnik, O., Spieler, O., Scheu, B., Dingwell, D.B., 2005. Permeability and degassing of dome lavas undergoing rapid decompression: an experimental determination. *Bull. Volcanol.* 67, 526–538.
- Mueller, S., Scheu, B., Spieler, O., Dingwell, D.B., 2008. Permeability control on magma fragmentation. *Geology* 36, 399–402.
- Namiki, A., Manga, M., 2005. Response of a bubble bearing viscoelastic fluid to rapid decompression: implications for explosive volcanic eruptions. *Earth Planet. Sci. Lett.* 236, 269–284.
- Namiki, A., Manga, M., 2008. Transition between fragmentation and permeable outgassing of low viscosity magmas. *J. Volcanol. Geotherm. Res.* 169, 48–60.
- Nathenson, M., Donnelly-Nolan, J.M., Champion, D.E., Lowenstern, J.B., 2007. *Chronology of Postglacial Eruptive Activity and Calculation of Eruption Probabilities for Medicine Lake Volcano, Northern California*. U.S. Geological Survey Scientific Investigations Report 5174-B, 10.
- Newman, S., Stolper, E.M., Epstein, S., 1986. Measurement of water in rhyolitic glasses: calibration of an infrared spectroscopic technique. *Am. Mineral.* 71, 1527–1541.
- Newman, S., Epstein, S., Stolper, E., 1988. Water, carbon dioxide, hydrogen isotopes in glasses from the ca. 1304 AD eruption of the Mono craters, California: constraints on degassing phenomena and initial volatile content. *J. Volcanol. Geotherm. Res.* 35, 75–96.
- Newman, S., Lowenstern, J.B., 2002. VOLATILECALC: a silicate melt–H<sub>2</sub>O–CO<sub>2</sub> solution model written in Visual Basic for Excel. *Comput. Geosci.* 28, 597–604.
- Ni, H., Zhang, Y., 2008. H<sub>2</sub>O diffusion models in rhyolitic melt with new high pressure data. *Chem. Geol.* 250, 68–78.
- Ni, H., Liu, Y., Wang, L., Zhang, Y., 2009a. Water speciation and diffusion in haploandesitic melts at 743–873 K and 100 MPa. *Geochim. Cosmochim. Acta* 73, 3630–3641.
- Ni, H., Behrens, H., Zhang, Y., 2009b. Water diffusion in dacitic melt. *Geochim. Cosmochim. Acta* 73, 3642–3655.
- Nolan, G., Bindeman, I., Experimental investigation of rates and mechanisms of isotope exchange (O, H) between volcanic ash and isotopically-labeled water. *Geochim. Cosmochim. Acta*, <http://dx.doi.org/10.1016/j.gca.2013.01.020>, in press.
- Okumura, S., Nakamura, M., Takeuchi, S., Tsuchiyama, A., Nakano, T., Uesugi, K., 2009. Magma deformation may induce non-explosive volcanism via degassing through bubble networks. *Earth Planet. Sci. Lett.* 281 (3–4), 267–274.
- Pallister, J.S., Hoblitt, J.S., Meeker, G.P., Newhall, C.G., Knight, R.J., Siems, D.F., 1996. Magma mixing at Mount Pinatubo volcano: petrographic and chemical evidence from the 1991 deposits. In: Newhall, C.G., Punongbayan, R.S. (Eds.), *Fire*

- and Mud: Eruptions and Lahars of Mount Pinatubo, Philippines. University of Washington Press, Seattle, pp. 687–731.
- Papale, P., 1997. Modeling of the solubility of a one-component H<sub>2</sub>O or CO<sub>2</sub> fluid in silicate liquids. *Contrib. Mineral. Petrol.* 126, 237–251.
- Papale, P., 1999. Modeling of the solubility of a two-component H<sub>2</sub>O+CO<sub>2</sub> fluid in silicate liquids. *Am. Mineral.* 84, 477–492.
- Papale, P., Moretti, R., Barbato, D., 2006. The compositional dependence of the saturation surface of H<sub>2</sub>O+CO<sub>2</sub> fluids in silicate melts. *Chem. Geol.* 229, 78–95.
- Polacci, M., Papale, P., Rosi, M., 2001. Textural heterogeneities in pumices from the climactic eruption of Mount Pinatubo, 15 June 1991, and implications for magma ascent dynamics. *Bull. Volcanol.* 63, 83–97.
- Polacci, M., Baker, D.R., Bai, L.P., Mancini, L., 2008. Large vesicles record pathways of degassing at basaltic volcanoes. *Bull. Volcanol.* 70 (9), 1023–1029.
- Princen, H., 1979. Highly concentrated emulsions Part I. *J. Colloid Interface Sci.* 71, 55–66.
- Proussevitch, A.A., Sahagian, D.L., Anderson, A.T., 1993. Dynamics of diffusive bubble growth in magmas: isothermal case. *J. Geophys. Res.* 98 (12), 22283–22307.
- Rogers, A.K., Duke, D., 2011. An archaeologically validated protocol for computing obsidian hydration rates from laboratory data. *J. Archaeol. Sci.* 38, 1340–1345.
- Rosi, M., Santacroce, R., 1983. The A.D. 472 “Pollena” eruption: a poorly-known Plinian event in the recent history of Vesuvius. In: Sheridan, M.F., Barberi, F. (Eds.), *Explosive Volcanism. Journal of Volcanology Geothermal Research* vol. 17, pp. 249–271.
- Ross, C.S., Smith, R.L., 1955. Water and other volatiles in volcanic glasses. *Am. Mineral.* 40, 1071–1089.
- Rouliia, M., Chassapis, K., Kapoutsis, J.A., Kamitsos, E.I., Savvidis, T., 2006. Influence of thermal treatment on the water release and the glassy structure of perlite. *J. Mater. Sci.* 41, 5870–5881.
- Rust, A.C., Cashman, K.V., 2004. Permeability of vesicular silicic magma: inertial and hysteresis effects. *Earth Planet. Sci. Lett.* 228, 93–107.
- Rust, A.C., Cashman, K.V., Wallace, P., 2004. Magma degassing buffered by vapor flow through brecciated conduit margins. *Geology* 32 (4), 349–352.
- Rust, A.C., Cashman, K.V., 2011. Permeability controls on expansion and size distributions of pyroclasts. *J. Geophys. Res.* 116, B11202.
- Rutherford, M.J., Sigurdsson, H., Carey, S., Davis, A., 1985. The May 18, 1980, eruption of Mount St. Helens 1. Melt composition and experimental phase equilibria. *J. Geophys. Res.* 90, 2929–2947.
- Saar, M.O., Manga, M., 1999. Permeability porosity relationship in vesicular basalts. *Geophys. Res. Lett.* 26, 111–114.
- Sahimi, M., 1994. *Applications of Percolation Theory*. Taylor and Francis, London, pp. 258.
- Schiano, P., 2003. Primitive mantle magmas recorded as silicate melt inclusions in igneous minerals. *Earth Sci. Rev.* 63 (1–2), 121–144.
- Shea, T., Gurioli, L., Houghton, B.F., 2012. Transitions between fall phases and pyroclastic density currents during the AD 79 eruption at Vesuvius: building a transient conduit model from the textural and volatile record. *Bull. Volcanol.* 74 (10), 2363–2368.
- Silver, L., Stolper, E., 1985. A thermodynamic model for hydrous silicate melts. *J. Geol.* 93, 161–178.
- Sobolev, A.V., 1996. Melt inclusions in minerals as a source of principle petrological information. *Petrology* 4, 209–220.
- Sparks, R.S.J., 1978. The dynamics of bubble formation and growth in magmas: a review and analysis. *J. Volcanol. Geotherm. Res.* 3 (1–2), 1–37.
- Sparks, R.S.J., 2003. *Dynamics of Magma Degassing*, 213. Geological Society, London, Special Publications 5–22.
- Spieler, O., Kennedy, B., Kueppers, U., Dingwell, D.B., Scheu, B., Taddeucci, J., 2004. The fragmentation threshold of pyroclastic rocks. *Earth Planet. Sci. Lett.* 226 (1–2), 139–148.
- Sterpenich, J., Libourel, G., 2006. Water diffusion in silicate glasses under natural weathering conditions: evidence from buried medieval stained glasses. *J. Non-Cryst. Solids* 352, 5446–5451.
- Stasiuk, M.V., Barclay, J., Carroll, M.R., Jaupart, C., Ratté, J.C., Sparks, R.S.J., Tait, S.R., 1996. Degassing during magma ascent in the Mule Creek vent (USA). *Bull. Volcanol.* 58, 117–130.
- Stevenson, C.M., Abdelrehim, I., Novak, S.W., 2004. High precision measurement of obsidian hydration layers on artifacts from the Hopewell site using secondary ion mass spectrometry. *Am. Antiquity* 69 (3), 555–567.
- Stevenson, J.A., Smellie, J.S., McGarvie, D., Gilbert, J.S., Cameron, B., 2009. Subglacial intermediate volcanism at Kerlingarfjöll, Iceland: magma–water interactions beneath thick ice. *J. Volcanol. Geotherm. Res.* 185, 337–351.
- Stevenson, C.M., Novak, S.W., 2011. Obsidian hydration dating by infrared spectroscopy: method and calibration. *J. Archaeol. Sci.*, 1716–1726.
- Takeuchi, S., Nakashima, S., Tomiya, A., Shinohara, H., 2005. Experimental constraints on the low gas permeability of vesicular magma during decompression. *Geophys. Res. Lett.* 32, L10312.
- Takeuchi, S., Nakashima, S., Tomiya, A., 2008. Permeability measurements of natural and experimental volcanic materials with a simple permeameter: toward an understanding of magmatic degassing processes. *J. Volcanol. Geotherm. Res.* 177, 329–339.
- Takeuchi, S., Tomiya, A., Shinohara, H., 2009. Degassing conditions for permeable silicic magmas: implications from decompression experiments with constant rates. *Earth Planet. Sci. Lett.* 283 (1–4), 101–110.
- Thomas, N., Jaupart, C., Vergnolle, S., 1994. On the vesicularity of pumice. *J. Geophys. Res.* 99, 15633–15644.
- Toramaru, A., 1990. Measurement of bubble size distributions in vesiculated rocks with implications for quantitative estimates of eruption processes. *J. Volcanol. Geotherm. Res.* 43, 71–90.
- Tuffen, H., Owen, J., Denton, J.S., 2010. Magma degassing during subglacial eruptions and its use to reconstruct palaeo-ice thicknesses. *Earth Sci. Rev.* 99, 1–18.
- Villemant, B., Michaud, V., Metrich, N., 1993. Wall rock-magma interactions in Etna (Sicily) studied by U–Th disequilibrium and REE systematics. *Geochim. Cosmochim. Acta* 57, 1169–1180.
- Villemant, B., Boudon, G., 1999. H<sub>2</sub>O and halogen (F, Cl, Br) behaviour during shallow magma degassing processes. *Earth Planet. Sci. Lett.* 168, 271–286.
- Wallace, P.J., 2005. Volatiles in subduction zone magmas; concentrations and fluxes based on melt inclusion and volcanic gas data. *J. Volcanol. Geotherm. Res.* 140 (1–3), 217–240.
- Walsh, S.D.C., Saar, M.O., 2008. Magma yield stress and permeability: insights from multiphase percolation theory. *J. Volcanol. Geotherm. Res.* 177 (4), 1011–1019.
- Watkins, J.M., Manga, M., De Paolo, D.J., 2012. Bubble geobarometry: a record of pressure changes, degassing, and regassing at Mono Craters, California. *Geology* 40, 699–702.
- Westrich, H.R., Stockman, H.W., Eichelberger, J.C., 1988. Degassing of rhyolitic magma during ascent and emplacement. *J. Geophys. Res.* 93, 6503–6511.
- Westrich, H.R., Eichelberger, J.C., 1994. Gas transport and bubble collapse in rhyolitic magma: an experimental approach. *Bull. Volcanol.* 56, 447–458.
- Wilson, L., 1980. Relationships between pressure, volatile content and ejecta velocity in three types of volcanic explosion. *J. Volcanol. Geotherm. Res.* 8, 297–313.
- Wohletz, K., Orsi, G., de Vita, S., 1995. Eruptive mechanism of the Neapolitan Yellow Tuff interpreted from stratigraphic, chemical and granulometric data. *J. Volcanol. Geotherm. Res.* 67, 263–290.
- Woods, A.W., Koyaguchi, T., 1994. Transitions between explosive and effusive eruption of silicic magmas. *Nature* 370, 631–645.
- Wright, H.M.N., Cashman, K.V., Rosi, M., Cioni, R., 2007. Bread-crust bombs as indicators of Vulcanian eruption dynamics at Guagua Pichincha volcano, Ecuador. *Bull. Volcanol.* 69 (3), 281–300.
- Wright, H.M.N., Weinberg, R.F., 2009. Strain localization in vesicular magma: implications for rheology and fragmentation. *Geology* 37 (11), 1023–1026.
- Wright, H.M.N., Cashman, K.V., Gottesfeld, E.H., Roberts, J.J., 2009. Pore structure of volcanic clasts: Measurements of permeability and electrical conductivity. *Earth Planet. Sci. Lett.* 280 (1–4), 93–104.
- Yokoyama, T., Okumura, S., Nakashima, S., 2008. Hydration of rhyolitic glass during weathering as characterized by IR microspectroscopy. *Geochim. Cosmochim. Acta* 72, 117–125.
- Yoshimura, S., Nakamura, M., 2008. Diffusive dehydration and bubble resorption during open-system degassing of rhyolitic melts. *J. Volcanol. Geotherm. Res.* 178 (1), 72–80.
- Yoshimura, S., Nakamura, M., 2010. Chemically driven growth and resorption of bubbles in a multivolatile magmatic system. *Chem. Geol.* 276, 18–28.
- Zhang, Y., 1999. H<sub>2</sub>O in rhyolitic glasses and melts: measurement, speciation, solubility, and diffusion. *Rev. Geophys.* 37, 493–516.
- Zhang, Y., Xu, Z., Zhu, M., Wang, H., 2007. Silicate melt properties and volcanic eruptions. *Rev. Geophys.* 45, RG4004.
- Zhang, Y., Ni, H., 2010. Diffusion of H, C, and O components in silicate melts. *Rev. Mineral. Geochem.* 72, 171–225.